

AXIAL CAPACITY OF PILES SUPPORTED ON INTERMEDIATE GEOMATERIALS

FHWA/MT-08-008/8117-32

Final Report

prepared for
THE STATE OF MONTANA
DEPARTMENT OF TRANSPORTATION

in cooperation with
THE U.S. DEPARTMENT OF TRANSPORTATION
FEDERAL HIGHWAY ADMINISTRATION

September 2008

prepared by
Robert Mokwa
Heather Brooks

Civil Engineering Department
Western Transportation Institute
Montana State University-Bozeman



RESEARCH PROGRAMS

Montana Department of Transportation



You are free to copy, distribute, display, and perform the work; make derivative works; make commercial use of the work under the condition that you give the original author and sponsor credit. For any reuse or distribution, you must make clear to others the license terms of this work. Any of these conditions can be waived if you get permission from the sponsor. Your fair use and other rights are in no way affected by the above.

Axial Capacity of Piles Supported on Intermediate Geomaterials

Final Project Report

Prepared by:

Dr. Robert Mokwa, P.E.

Associate Professor, Civil Engineering Department

and

Heather Brooks

Graduate Student, Civil Engineering Department

of the

College of Engineering/Western Transportation Institute
Montana State University - Bozeman

Prepared for:

State of Montana
Department of Transportation
Research Programs

in cooperation with the

U.S. Department of Transportation
Federal Highway Administration

September 2008

TECHNICAL REPORT DOCUMENTATION PAGE

1. Report No.: FHWA/MT-08-008/8117-32	2. Government Access No.:	3. Recipient's Catalog No.:	
4. Title and Subtitle: Axial Capacity of Piles Supported on Intermediate Geomaterials		5. Report Date: September 2008	
		6. Performing Organization Code:	
7. Author(s): Robert Mokwa and Heather Brooks		8. Performing Organization Report Code:	
9. Performing Organization Name and Address: Montana State University/Western Transportation Institute Civil Engineering Dept., Bozeman, Montana 59717		10. Work Unit No.:	
		11. Contract or Grant No.: 8117-32	
12. Sponsoring Agency Name and Address: Research Programs Montana Department of Transportation 2701 Prospect Avenue Helena, Montana 59620-1001		13. Type of Report and Period Covered: Final Report March 2006 – September 2008	
		14. Sponsoring Agency Code: 5401	
15. Supplementary Notes: Research performed in cooperation with the Montana Department of Transportation and the U.S. Department of Transportation, Federal Highway Administration. This report can be found at http://www.mdt.mt.gov/research/docs/research_proj/axial/final_report.pdf .			
16. Abstract: <p>The natural variability of intermediate geomaterials (IGMs) exacerbates uncertainties in deep foundation design and may ultimately increase construction costs. This study was undertaken to investigate the suitability of conventional pile capacity formulations to predict the axial capacity of piles driven into IGM formations. Data from nine Montana Department of Transportation bridge projects were collected, compiled, and analyzed. Axial pile analyses were conducted using a variety of existing methods and computer programs, including: DRIVEN, GRLWEAP, FHWA Gates driving formula, WSDOT Gates driving formula, and an empirical method used by the Colorado Department of Transportation. The results of the analyses were compared to pile capacities determined using PDA measurements obtained during pile driving and wave equation analyses conducted using the CAPWAP program.</p> <p>The capacity comparisons clearly demonstrated the inherent variability of pile resistance in IGMs. Most of the projects exhibited considerable variation between predicted capacities calculated using DRIVEN and measured CAPWAP capacities. For example, five of the six restrike analyses were over predicted using DRIVEN, one by as much as 580%. The majority of shaft capacity predictions for cohesionless IGMs were less than the measured CAPWAP capacities; the worse case was a 400% under prediction (a factor of 5). Toe capacity predictions were also quite variable and random, with no discernable trends. This study indicates that traditional semiempirical methods developed for soil may yield unreliable predictions for piles driven into IGM deposits. The computed results may have little to no correlation with CAPWAP capacities measured during pile installation. Currently, CAPWAP capacity determinations during pile driving or static load tests represent the only reliable methods for determining the capacity of piles driven into IGM formations.</p>			
17. Key Words: Intermediate Geomaterial, IGM, pile axial capacity, CAPWAP analyses		18. Distribution Statement: No restrictions. This document is available through National Tech. Info. Service, Springfield, VA 22161.	
19. Security Classif. (of this report): Unclassified	20. Security Classif. (of this page): Unclassified	21. No. of Pages: 89	22. Price:

DISCLAIMER STATEMENT

This document is disseminated under the sponsorship of the Montana Department of Transportation and the United States Department of Transportation in the interest of information exchange. The State of Montana and the United States Government assume no liability of its contents or use thereof.

The contents of this report reflect the views of the authors, who are responsible for the facts and accuracy of the data presented herein. The contents do not necessarily reflect the official policies of the Montana Department of Transportation or the United States Department of Transportation.

The State of Montana and the United States Government do not endorse products of manufacturers. Trademarks or manufacturers' names appear herein only because they are considered essential to the object of this document.

This report does not constitute a standard, specification, or regulation.

ALTERNATIVE FORMAT STATEMENT

MDT attempts to provide accommodations for any known disability that may interfere with a person participating in any service, program, or activity of the Department. Alternative accessible formats of this information will be provided upon request. For further information, call (406) 444-7693, TTY (800) 335-7592, or Montana Relay at 711.

ACKNOWLEDGEMENTS

The authors gratefully acknowledge the valuable assistance provided by the MDT Geotechnical Section in gathering and providing project records for the analyses conducted herein.

Acknowledgement of financial support for this research is extended to the Montana Department of Transportation and the Research and Innovative Technology Administration (RITA) at the United States Department of Transportation through the Western Transportation Institute at Montana State University.

EXECUTIVE SUMMARY

Deep foundations are relatively expensive and can constitute a significant percentage of the overall cost on bridge projects. Uncertainties in subsurface conditions can result in higher construction costs due to higher factors of safety in design, higher construction bids, and higher frequency of contractor claims. The natural variability of IGMs exacerbates uncertainties in deep foundation design and may ultimately increase construction costs. This study was undertaken to find a reliable relationship between pile resistance and IGM properties.

For the analyses conducted in this study, IGMs were divided into two broad categories, cohesive and cohesionless. Cohesive IGMs have an intrinsic bonding or cohesion within their structure; for example, claystone, sandstone and siltstone. Cohesionless IGMs are very dense materials, often sandy gravels, which do not contain any bonding between the particulates.

IGM data and information from nine Montana Department of Transportation construction projects were collected, compiled, and analyzed. CAPWAP information was obtained from reports completed for each project. Axial pile analyses were conducted using a variety of existing methods and computer programs, including: DRIVEN, GRLWEAP, FHWA Gates driving formula, WSDOT Gates driving formula, and an empirical method used by the Colorado Department of Transportation. The results of the analyses were compared to pile capacities determined using PDA measurements obtained during pile driving and wave equation analyses conducted using the CAPWAP program.

The methodology behind this research was iterative. Evaluations were conducted by creating parametric comparisons to search for trends or useful relationships within the available information. The variability of IGM materials provided an interesting challenge because of the unpredictable response of the material to pile driving and because of the many variables involved with pile driving and pile resistance.

Case studies in which a CAPWAP analysis and a static load test were conducted on the same project were compiled into a database. From this information, it was determined that the CAPWAP dynamic capacity is well correlated to static load test

capacities for piles driven into soil and IGM deposits. Consequently, the CAPWAP capacity was used as a baseline comparison in this study.

The capacity comparisons evaluated using measured data from nine Montana bridge projects clearly demonstrated the inherent variability of pile resistance in IGMs. Most of the projects exhibited considerable variation between predicted capacities calculated using DRIVEN and the measured CAPWAP capacity. For example, five of the six restrike analyses were over predicted using DRIVEN, one by as much as 580%. In these projects, the shaft resistance was under predicted in 12 out of 20 occurrences in cohesive IGMs; however, there were outliers in which capacity was over predicted by 150% to 380%. The majority of shaft capacity predictions for cohesionless IGMs were less than the measured CAPWAP capacities; the worse case was a 400% under prediction (a factor of 5). Toe capacity predictions were also quite variable and random, with no discernable trends. In general, the predicted capacities determined from DRIVEN and GRLWEAP were in relatively good agreement; however, neither accurately matched the measured CAPWAP capacities.

During design, careful consideration should be given to evaluating pile stresses and potential pile damage if IGM formations are expected at the site. It may be prudent to use a range of IGM strength parameters (parametric study) in this evaluation because of the variable nature of these materials and the real potential for excessively strong and excessively weak anomalies within the IGM deposit.

In summary, a static load test represents the most accurate method for determining the axial capacity of a pile driven into an IGM deposit. PDA measurements with CAPWAP analyses provide the next most reliable option at a lower cost. Based on the data analyzed in this the study, it appears that the WSDOT Gates formula may be the best alternative to use as a check of CAPWAP results or as an approximate estimate of capacity during pile driving.

IGMs are incredibly varied materials in which current geological and geotechnical knowledge provide engineers with only a limited understanding of their properties and behavior. To decrease uncertainties and thus construction costs, further testing and research is needed to improve the state of practice of deep foundation design in IGMs.

TABLE OF CONTENTS

1 INTRODUCTION 1

2 OVERVIEW OF INTERMEDIATE GEOMATERIALS 3

 2.1 General Description of IGMs 3

 2.2 IGM Strength 4

 2.3 Properties of IGMs..... 6

 2.4 IGMs in Montana..... 8

 2.5 Sampling and Testing Methods 9

 2.6 Foundation Design Experience in IGMs 11

3 BACKGROUND OF ANALYTICAL METHODS 12

 3.1 DRIVEN 13

 3.2 Stress-Wave Theory..... 14

 3.3 GRLWEAP 15

 3.4 CAPWAP..... 17

 3.5 Colorado Department of Transportation Method 19

4 PROJECT SUMMARIES 20

5 ANALYSIS OF PROJECT DATA..... 27

 5.1 Evaluate Accuracy of Current Design Procedures 28

 5.2 Investigation of Possible Correlations 31

 5.2.1 Normalized Capacity Comparisons 31

 5.2.2 Iterative Solutions 35

 5.3 Accuracy of Other Capacity Prediction Methods 38

6 SUMMARY AND CONCLUSIONS 46

REFERENCES CITED 50

 Appendix A: Project Subsurface Profiles 58

 Appendix B: Compiled Project Data 69

 Appendix C: Comparison of Test Results from the Literature 75

LIST OF TABLES

Table 2.1. Definition of IGM by Author..... 6

Table 3.1. Parametric Study of GRLWEAP Quake and Damping Parameters 16

Table 4.1. Projects Analyzed in this Study 21

Table 4.2. Project Construction Summaries - IGM Strength..... 23

Table 4.3. Project Construction Summaries - Design vs. Actual Construction..... 24

Table 4.4. Computed Stresses within Piles During Driving 26

LIST OF FIGURES

Figure 2.1. IGM formation processes. 4

Figure 2.2. Map of project locations and IGM types. 8

Figure 3.1. Diagrammatic summarization of computer programs and capacity analysis methods. 12

Figure 3.2. Comparison of static load test and CAPWAP capacities from the literature.
 (a) Full scale plot of all data. (b) Data points at lower capacities. 18

Figure 5.1. Comparison of predicted total capacity to measured CAPWAP capacity. ... 29

Figure 5.2. Comparison of predicted shaft capacity to measured CAPWAP shaft capacity. 30

Figure 5.3. Comparison of predicted toe capacity to measured CAPWAP toe capacity. 30

Figure 5.4. Normalized shaft resistance compared to pile length in IGM. 33

Figure 5.5. Normalized shaft resistance with project number designation. 33

Figure 5.6. Comparison of normalized toe resistance with unconfined compression strength of cohesive IGMs. 34

Figure 5.7. Comparison of normalized toe resistance with length of pile in IGM. 35

Figure 5.8. Strength multiplier use to match measured CAPWAP capacities. 36

Figure 5.9. Comparison of M required for a CAPWAP capacity match to the pile length in IGMs. 37

Figure 5.10. Comparison of M required for a CAPWAP capacity match to the measured CAPWAP capacity. 37

Figure 5.11. Comparison of the calculated WSDOT Gates capacities to the measured CAPWAP capacity. 39

Figure 5.12. Comparison of capacity calculations in cohesive IGMs. (a) Full scale. (b) Detail at lower capacities. 41

Figure 5.13. Comparison of capacity calculations in cohesionless IGMs. (a) Full scale. (b) Detail of points at lower capacities. 42

Figure 5.14. Comparison of capacity calculations in cohesive IGMs compared by project number and bent. 43

Figure 5.15. Comparison of capacity calculations in cohesionless IGMs compared by project bent.....	44
Figure A.1. Soil profile for project Q744 – Medicine Tree.....	59
Figure A.2. Soil profile for project 1744 (Vicinity of White Coyote Creek) main structure.....	60
Figure A.3. Soil profile for project 2144 (Nashua Creek) main structure.....	61
Figure A.4. Soil profile for project 2144 (Nashua Creek) overflow structure.....	62
Figure A.5. Soil profile for project 3417 (West Fork Poplar River) main structure.....	63
Figure A.6. Soil profile for project 3417 (West Fork Poplar River) overflow structure.....	64
Figure A.7. Soil profile for project 4226 (Goat Creek) main structure.....	65
Figure A.8. Soil profile for project 4230 (Bridger Creek) main structure.....	66
Figure A.9. Soil profile for project 4239 (Big Muddy Creek) main structure.....	67
Figure A.10. Soil profile for project 4244 (Keyser Creek) main structure.....	68

1 INTRODUCTION

Pile foundations are designed and installed to sustain axial and lateral loads without bearing capacity failure or excessive settlement. Axial resistance is developed from a combination of friction or adhesion along the pile shaft and bearing resistance at the pile tip. Bridge foundations within the state of Montana are often founded on driven piles because of their high axial and lateral capacity and their resistance to scour and settlement. During the design phase of a project, geotechnical engineers use the computer programs DRIVEN (2001) and GRLWEAP (2005) to estimate the axial capacity of driven piles. The computer program DRIVEN is used to calculate the axial capacity of a pile based on soil strength characteristics using semiempirical formulations. The computer program GRLWEAP is used to assist the designer in selecting the pile driving hammer and system, and to estimate the response of the pile during driving.

Piles are driven into soil, rock, and in some cases into materials that are situated within the continuum bracketed by soil and rock. In recent technical literature, these materials have been classified using the term intermediate geomaterials (IGMs). In the past, other names have been used for IGMs, including: formation materials, indurated soils, soft rocks, weak rocks, and hard soils.

Field measurements obtained during pile installation using the Pile Dynamic Analyzer (PDA) indicate that on many projects in which IGMs are encountered, the capacity of the piles is often quite different than predicted. Piles driven into IGMs may stop short of the anticipated design elevation (premature refusal) or they may require driving to greater depth (known as running) to achieve the required capacity. IGMs do not behave the same as soils when disturbed during pile installation and then subsequently loaded. Modern analytical methods and computer programs for predicting axial capacity and driving behavior of piles in soil may not be adequate for use in IGM formations.

Because the behavior of piles founded in IGMs is not well known, Montana Department of Transportation (MDT) often requires a PDA test to evaluate the pile axial capacity in the field. PDAs are conducted during pile driving (or restrrike) by attaching

accelerometers and strain gages to the pile. Pulses of stress that travel down the length of the pile and reflect upward are monitored and are used to determine the capacity using a closed-form solution to the stress-wave equation. Signal matching techniques incorporated in the Case Pile Wave Analysis Program (CAPWAP 2006) can be used to further refine the analyses. Static load tests are generally recognized as the most accurate approach for measuring pile capacity. Static load tests involve driving reaction piles and the use of relatively complex monitoring systems. While accurate, this type of testing is relatively expensive.

The purpose of this study was to determine if an improved method of analysis could be employed to evaluate the capacity of piles driven into IGM formations using information and data obtained from nine MDT bridge projects. A large quantity of information from project files was reviewed and synthesized in this study, including:

- DRIVEN reports,
- CAPWAP summary reports,
- end-of-driving blow counts,
- GRLWEAP results, and
- project foundation reports.

Subsurface profiles for each project are provided in Appendix A and tabulated data from the projects are provided in Appendix B. Analyses were conducted to evaluate the accuracy of capacity prediction methods and to assess trends within the measured dynamic capacity test results.

2 OVERVIEW OF INTERMEDIATE GEOMATERIALS

2.1 General Description of IGMs

Intermediate geomaterials (IGMs) reside at the center of a continuum between soil and rock; consequently, principles from both soil and rock mechanics apply to IGMs in terms of material behavior and design methodology. Papageorgiou (1993) theorizes that the analysis and design of piles within IGMs should include both a geologic component (focused on method of formation) and a geotechnical component (focused on the engineering response). The following quote from Gannon et al. (1999) provides an insightful description of weak rocks, which fits in well with the current view of IGMs:

“Weak rocks are either intrinsically weak (they have undergone a limited amount of gravitational compaction and cementation), or they are products of the disintegration of previously stronger rocks in a process of retrogression from being fully lithified and becoming weak through degradation, weathering and alteration.”

IGM formation processes fit into two basic categories: 1) soil has been strengthened to near rock-like characteristics, or 2) rock formations have been weakened to near soil-like levels. Within the scope of this investigation, there are two overriding types of IGMs, cohesive and cohesionless. Cohesive IGMs have an intrinsic component bonding; for example, siltstone, claystone, mudstone, sandstone, argillaceous (clay-based sedimentary rock), and arenaceous (sand-based sedimentary rock) materials. Cohesionless IGMs include very dense granular materials that derive strength predominately from frictional resistance rather than intrinsic particulate bonding.

Cohesive IGMs often contain clay particles, which can influence the electrochemical bonding that occurs on a microscopic level. Clay content of the in-situ material can significantly affect the behavior of the deposit when exposed to water. In one case described in the literature, a low clay content mudstone exhibited a collapsible behavior while a high clay content claystone exhibited expansive behavior (El-Sohby et al. 1993). In another instance, expansive behavior in a very dense clay IGM deposit

displayed swelling pressures greater than the overburden stresses within the lithology (Brouillette et al. 1993).

Cohesionless IGMs, by definition, have no intrinsic bonding. Consequently, geotechnical analysis methods are typically applied to determine the frictional characteristics of the particulates. Dense sandy gravels with silt are the most common type of cohesionless IGMs in Montana. It is theorized that these materials undergo significant dilation before failure, creating high friction angles. The term dilation in this context refers to the volume increase that occurs when a load is applied and the material subsequently expands as particles are displaced and re-arranged.

2.2 IGM Strength

The shear strength of IGMs is less than intact rock, but greater than soil. The strength range of IGMs is quite large because of the processes by which IGMs are formed. These processes are shown conceptually in Figure 2.1. IGMs occur when the natural processes of soil or rock formation are incomplete or interrupted. For example, in some settings the soil strengthening process (deposition followed by lithification, diagenesis or cementation) may be interrupted before the creation of rock. In other settings, IGMs are the byproduct of weakening processes (e.g., weathering and disintegration) of intact rock (Gannon et al. 1999).

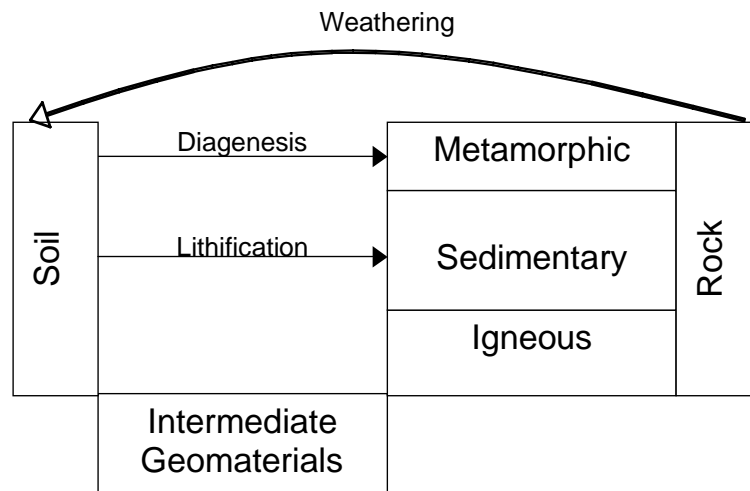


Figure 2.1. IGM formation processes.

Lithification is a formation process in which regolith (soil) is compressed causing pore water to slowly escape from the pores allowing bonding to form between the original particulates. Diagenesis is a metamorphic process in which there is a physical, chemical or biological change in the sediment causing bonding of particulates. Intrinsic weaknesses can form during these processes, which include: loose texture (poor bonding), the presence of cavities, and poor cementation (Tanimoto 1982, Oliveira 1993). Cavities within the matrix of an IGM can severely reduce strength and stiffness properties because of the loss of load transfer through void regions. Cementation is a process in which particles are bonded or cemented by salts as the pore water evaporates. IGMs formed during these soil-to-rock processes generally exhibit relatively loose texture and poor cementation bonding between particles.

Weathering is the process of strength reduction in rock masses, and is generally categorized as mechanical or chemical. Joints and fissures are formed during the mechanical weathering, which includes processes such as: reduction in overburden stress, thermal changes, tectonisation, and freeze thaw effects. Reduction in overburden stresses cause fracturing due to the release of pressure in the vertical direction. Tectonisation describes the formation of joints and fissures as a result of earthquake stresses and movements.

Weak or damaged component bonding is often the result of chemical weathering, which includes processes such as: dissolution, hydrolysis, oxidation, and carbonation. For example, carbonation causes the formation of carbonic acid, a common ingredient in acid rain, which dissolves limestone formations.

Because of their variability, the behavior of IGMs is far from predictable. Wide ranges of material behavior have resulted in a multitude of disparate definitions and descriptions of IGMs in the literature, which are primarily based on material strength. Table 2.1 summarizes definitions of IGMs from multiple sources, which used the unconfined compression value or the SPT N-value as a basis for distinguishing IGMs. A reasonable definition for most applications is that IGMs will have a uniaxial compressive

strength in the range of 600 to 12,500 kPa, an SPT N-value greater than 50 blows per 0.3 m, and a stiffness modulus in the range of 100 to 1,000 MPa. The wide range of published definitions is indicative of the variability of IGM geotechnical engineering properties.

Table 2.1. Definition of IGM by Author

Author (Year)	Type of IGM	Definition
Dobereiner and de Freitas (1986)	Sandstone	Saturated Unconfined Compression from 0.5-20 MPa
Finno and Budyn (1988)	All	Unconfined Compression 0.5-5 MPa SPT N-values >50 Blows/ 0.3 m
Johnston (1989)	All	Unconfined Compression >0.5 MPa
Akai (1993)	All	Unconfined Compression 1-10 MPa
Clarke and Smith (1993)	All	Unconfined Compression < 5MPa
de Freitas (1993)	Arenaceous*	Unconfined Compression 1-25 MPa
Geological Society of London (de Freitas 1993)	All	Unconfined Compression 1.25-5 MPa
International Society of Rock Mechanics (de Freitas 1993)	All	Unconfined Compression 5-25 MPa
Mayne and Harris (1993)	Cohesionless	SPT N-values > 50 blows/ 0.3 m
O'Neill et al (1996)	All	Unconfined Compression 0.5-5 MPa
Marinos (1997)	All	Undrained Cohesion > 0.3 MPa Unconfined Compression > 2 MPa
Gannon et al. (1999)	All	Unconfined Compression >0.6 MPa

*Arenaceous – sand-based sedimentary rock

2.3 Properties of IGMs

“IGM is heterogeneous, with many inhomogeneities, particularly over horizontal and vertical distances comparable to the length, breadth, and separation of pile sockets,” (Gannon et al. 1999). The variation in material strength over small distances emphasizes the need for geological and geotechnical considerations when evaluating IGM properties (Krauter 1993). Geological considerations include the formation method, jointing,

fissuring, and strength of the formation mass. Geotechnical considerations include the type of bonding between particulates and any frictional components.

There are two property characteristics to be considered when examining IGMs: 1) the formation mass geologic properties, which include joints and fissures and 2) constituent material properties, which apply to mechanical properties on a particulate level.

Geological components of IGMs are specifically related to the behavior of the formation mass. A rock formation can be weak due to the geometry of its joints and fissures or the material itself can be weak. For example, if the constituent rock is strong and the jointing geometry causes weakness, the formation will be weak. Of course, if the constituent rock is weak then the overall formation will also be weak. IGMs exhibit analogous behavior; that is, the material itself may be weak or the jointing characteristics may cause weakness. Constituent material properties are typically determined from tests on samples obtained from boreholes. These types of samples are useful for examining material index properties, but do not provide a good indication of jointing and fissuring.

The bonding between particulates in IGMs can be affected by external sources, including fresh water. For example, most cohesive IGMs degrade with exposure to water (Spink and Norbury 1993). Argillaceous IGMs, like mudstone and shale, are particularly prone to degradation. Observed strength losses of greater than 60% in shale and 40% in mudstone are not uncommon (Spink and Norbury 1993). de Freitas (1993) reports on measured strength losses of arenaceous (sand-based) IGMs when exposed to water.

In summary, the origins of IGM formations vary widely and deposits of IGMs often exhibit heterogeneities in material properties that change considerably both laterally and vertically over relatively small distances. Abrupt changes in subsurface conditions emphasize the value of both geological and geotechnical considerations when conducting a site evaluation where IGMs are suspected. From a geologic perspective, IGM strength is controlled by the strength of the bonded geomaterial and the impacts of jointing and fissuring. Geotechnical considerations include an evaluation of chemical and mechanical bonding forces that contribute to IGM strength. Because the bonding processes are not

complete, intrinsic weaknesses within a formation may exist, which can be further exacerbated by the intrusion of water.

2.4 IGMs in Montana

IGMs typically encountered in Montana include materials that are categorized as cohesive and cohesionless. Cohesive IGMs encountered in Montana include shale, claystone, siltstone, and sandstone. Cohesionless IGMs primarily consist of deposits of very dense sandy gravels with varied quantities of silt. Figure 2.2 contains a map showing the MDT project sites examined in this study, with the corresponding IGM type.

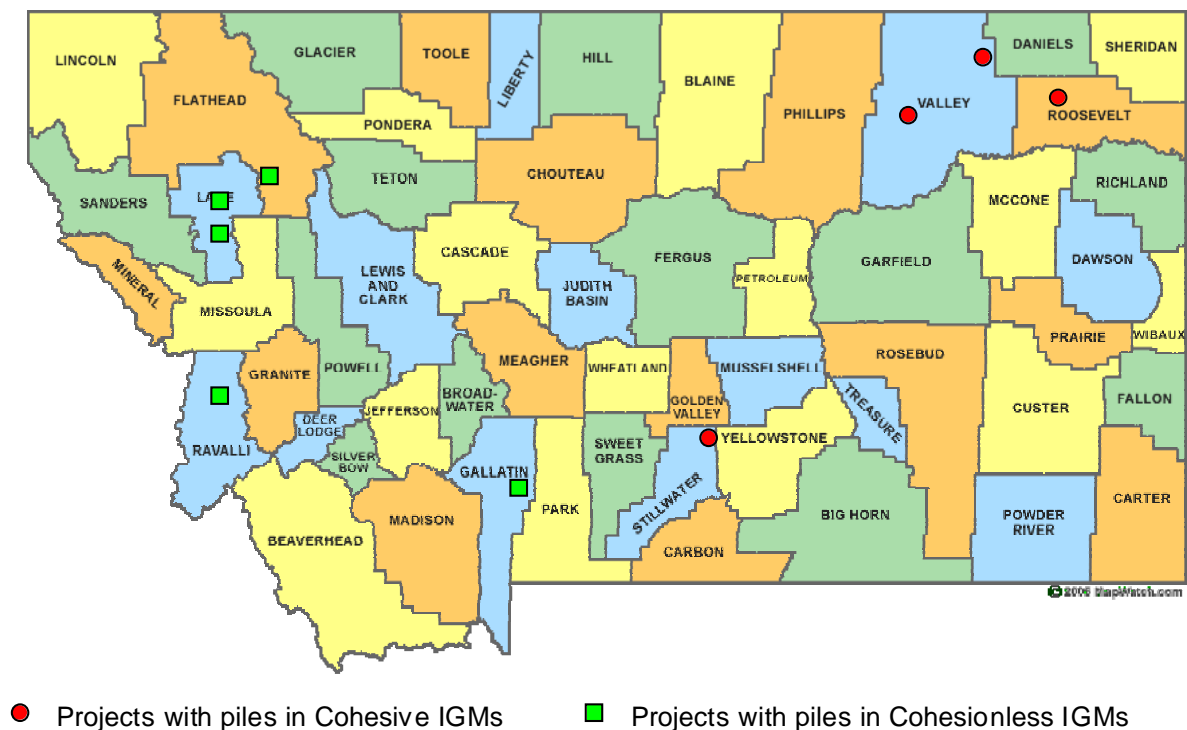


Figure 2.2. Map of project locations and IGM types.

2.5 Sampling and Testing Methods

Unconfined compression testing is the most common laboratory method for estimating the strength of IGM samples. Unconfined compression testing is a form of triaxial testing in which the cell or confining pressure is zero gage or atmospheric. The unconfined compression test is most often used because of its relative simplicity and the ability of the device to apply a wide range of piston loads, which is necessary for testing IGMs. Soil triaxial equipment does not typically have the loading capacity to test IGM samples or the displacement measurement sensitivity to determine the stiffness and strength properties of IGMs.

Standard penetration testing (SPT) and rock coring are the most common methods for sampling IGMs. However, neither method provides relatively undisturbed samples for laboratory strength and compressibility testing. Problems with SPT testing in IGM formations include: damaged split spoon samplers, skewed SPT N-values, and severely disturbed samples or no sample recovery. Rock coring can be used with varied success at obtaining disturbed IGM samples. However, IGMs typically have very poor rock quality designation and core recoveries can vary from 0 to 100% depending on IGM strength and formation characteristics. Drilling fluid can impact the observed strength properties of the IGM, as noticed with the impact of water on mudstone and shale. Cripps and Taylor (1981) suggest that block sampling can yield reliable laboratory testing results. They concluded that the specimen orientation significantly affects the observed strength of the material; that is, IGMs tend to exhibit anisotropic strength characteristics. Unfortunately, block sampling is not usually practical or economical on most projects. Solutions to the difficult sampling process will require more research and further ingenuity.

Testing IGMs in their natural in-situ condition is preferable to laboratory testing because of the aforementioned sampling issues and laboratory testing inaccuracies. Plate load tests and pressuremeter tests have been described in the literature as potentially viable alternatives to SPT testing and rock coring. Johnston (1995) and Campos et al. (1993) report that plate load tests can be used to evaluate the stiffness properties of IGMs, even in deposits that contain defects such as joints and fissures. However, the test is not

practical for deposits at great depths, and the test is more expensive and time consuming than SPT testing and rock coring. Akai (1993) reports that pressuremeter testing can be used to provide relatively accurate strength and stiffness properties of IGM formations. Pressuremeter testing can be conducted in two ways; either the pressuremeter apparatus is placed into a pre-existing borehole or a special self-boring pressuremeter is used. Clarke and Smith (1993) recommend the self-boring pressuremeter because it can drill into a formation while minimizing changes to in-situ stresses or properties.

In summary, currently available sampling methods are not adequate for obtaining reasonably undisturbed samples of IGMs, and laboratory testing methods cannot fully correct for disturbances that inevitably occur when an IGM deposit is sampled using either soil or rock sampling techniques. Laboratory test results are approximate, at best, without high-quality undisturbed samples. Research conducted by de Freitas (1993) indicates that disparities between laboratory test results and in-situ test results increase as the strength of the IGM decreases. Consequently, the typical subsurface investigation and testing approach must be altered when an IGM deposit is expected within the zone of influence of the foundation. Gannon et al. (1999) expand on this theme:

“Early recognition of the presence of weak rock and the need for a piled foundation solution are essential for an effective site investigation to be planned and executed. For piling in weak rock, the investigation involves three broad considerations: nature, properties and behavior.”

Most subgrade investigations do not address IGMs as an independent material. Investigations are often focused on the overburden soil and the underlying bedrock but not the gray area in between (i.e., the IGM).

Gannon et al. (1999) postulate a systemic approach in which soil and rock sampling techniques are overlapped to provide a more accurate picture of the IGM. Their approach consists of the development of a model that includes the following components of information:

- regional and local site geology,
- project and site geometry,
- groundwater conditions,

- overburden soil properties,
- properties of the underlying rock, and
- predicted or anticipated behavior of the system.

This model has value as a general approach for developing an investigative plan and sampling program; however, it still lacks specifics in regards to IGM sampling and testing protocols.

2.6 Foundation Design Experience in IGMs

Most foundation research on IGMs has focused on drilled shafts and IGM material properties. Very limited published information is available on driven pile foundations in IGMs. This information is mostly general and does not provide specific design or analysis details.

The pile driving process may be one of the most influential factors affecting pile capacity. Foundations in IGMs are sensitive to the installation methods because the process of pile driving can alter IGM properties and the alteration can be difficult to measure (Gannon et al. 1999). Changes in IGM properties during pile driving can result in significant design inaccuracies. Because of these potential inaccuracies, Reeves et al. (1993) recommend conducting dynamic tests on at least one pile in each bent or group to ensure the required capacity has been obtained.

Pile axial capacity may not always control the design of the foundation. In some cases, design may be governed by serviceability requirements, like settlement. When serviceability requirements control the design in IGMs, O'Neill et al. (1996) recommend pressuremeter testing to more accurately estimate the settlement behavior.

3 BACKGROUND OF ANALYTICAL METHODS

Pile foundations are commonly used for bridges and buildings when the soil cannot support the applied loads without excessive settlement, or the scale and magnitude of loads cannot adequately be supported on shallow foundations. Most bridges require deep foundations due to the combination of loads and moments, and the potential for scour.

Computer programs are often used by engineers as analytical aids when designing deep foundations. Analyses and capacity evaluations using these programs can be divided into two general categories (with some overlap): 1) predictive methods and 2) capacity determinations, as shown in Figure 3.1. An overview of the analytical methods used in this study is provided in the following paragraphs.

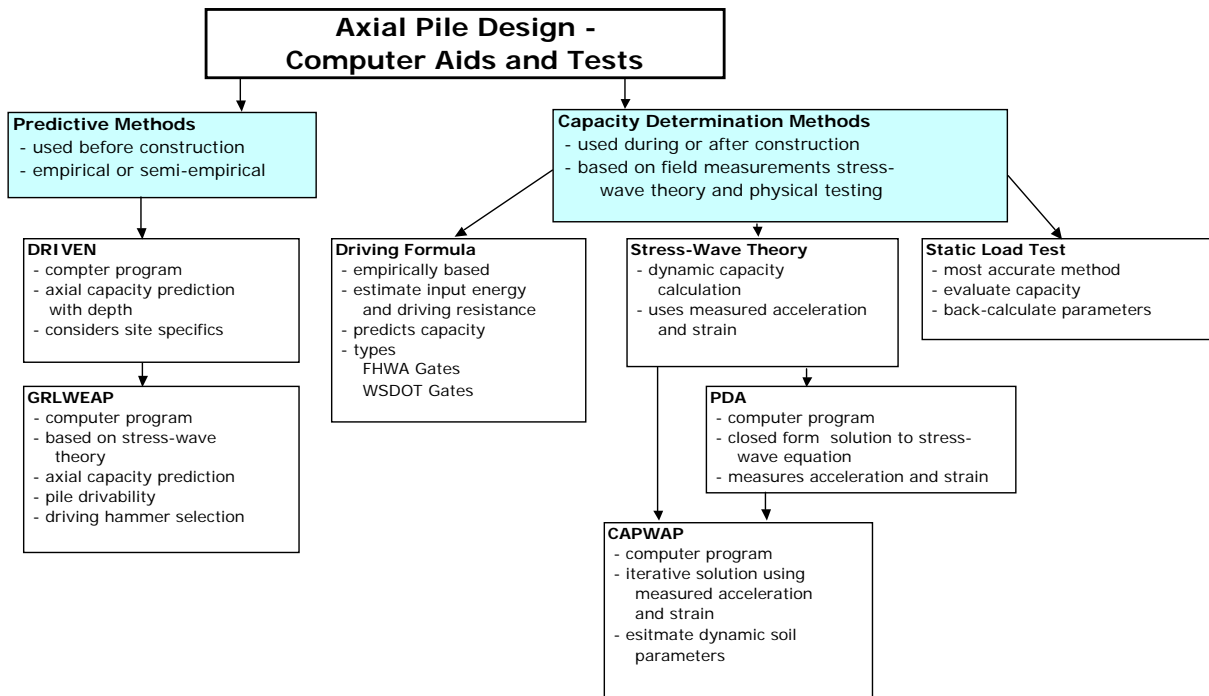


Figure 3.1. Diagrammatic summarization of computer programs and capacity analysis methods.

3.1 DRIVEN

The DRIVEN computer program was created by the Federal Highway Administration (FHWA) to calculate the axial capacity of driven piles. The DRIVEN program uses methods and equations presented in the FHWA Driven Pile Manual (2006). Input to the program can be SPT blow counts, or values of soil friction and cohesion. This software replaces the SPILE program that was developed by the FHWA in the 1980's. DRIVEN can accommodate multiple water tables, scour, soft compressible soil and negative skin friction, and can be used to create an input file for the GRLWEAP software.

For each layer of the lithology, soil strength parameters are entered for either cohesive or cohesionless soils. Inputs for cohesive IGMs include undrained shear strength (c_u) or a user defined adhesion (c_a). Adhesion is an empirically derived factor that relates undrained shear strength to frictional resistance per unit area. The relationship between adhesion and undrained shear strength is derived from Tomlinson's research as cited in (Mathias and Cribbs 1998). Cohesionless IGM inputs include SPT N-values or internal soil friction angles, for both side friction and end bearing. The Nordlund method is used to determine the capacity of piles in cohesionless layers (Mathias and Cribbs 1998).

The Tomlinson α method is used to calculate the shaft capacity of piles in cohesive soils. Shaft capacity is calculated by summing the product of the pile perimeter, the depth of the cohesive layer and the adhesion. Adhesion is estimated from the Tomlinson α approach using the following equation:

$$c_a = \alpha c_u \quad (1)$$

where, c_a is the adhesion, α is an empirical adhesion factor, and c_u is the undrained shear strength. The factor α is a function of the soil strength, in-situ effective stress, pile width and depth, and the texture of overlying soil layers (Das 2005). In the computer program DRIVEN, a simplified approach is employed in which c_a is directly correlated to c_u . For materials with high c_u values (e.g., cohesive IGMs with $c_u > 150$ kPa), the user can

directly input c_a to avoid limitations that the DRIVEN software places on the correlation between c_a and c_u , for large values of c_u .

3.2 Stress-Wave Theory

Many empirical formulas (dynamic formulas) have been developed to relate the end of driving blow count to the static capacity of driven piles. However, because the methods used to evaluate energy transfer are crude in these formulas, the solutions are approximate at best. The wave equation introduced by Smith (1960) represented a significant improvement to the level of complexity and reliability in evaluating the response of piles to the driving process.

The wave equation is used to track the movement of stress waves along a pile. A stress wave occurs when a force, like the blow of a hammer, impacts an object. The stress from the impact moves in a wave along the pile length. If the pile is bearing against a stiff or hard surface, like hard or very dense soil, the initial impact wave will rebound, either in whole or in part. Comparison of the initial wave to the rebound wave provides a measure of the energy removed from the wave by the movement of soil along the shaft and toe of the pile.

To facilitate analyses, a model was created to enable computer computation. In this model, the hammer impact represents the initial energy within the system. The energy flows through the hammer cushion, which is modeled as a spring. A percentage of the remaining energy continues through the helmet, modeled as a weight, and into the pile. The pile is represented as a series of weights and springs, each spring has a stiffness equal to the Young's modulus of the steel. The relative displacement of each weight is used to model the movement of the wave along the system.

During driving, energy loss within the soil is quantified using dynamic parameters referred to as quake and damping. Quake is the amount of displacement a pile undergoes before the soil yields plastically. Quake is represented by a spring in the wave equation model. Energy is removed from the system until the quake displacement is reached within the spring. Damping represents the amount of energy that is removed from the system as a result of the movement of soil along the shaft and at the toe of the pile. The

wave equation model is used within the calculations conducted by GRLWEAP and CAPWAP.

3.3 GRLWEAP

The computer program GRLWEAP simulates the behavior of a pile and the surrounding soil or rock under the impact of a pile driving hammer. The GRLWEAP software provides an estimation of dynamic pile stresses, bearing capacities, blow counts and installation time for a given hammer/pile system. The software contains a hammer database with over 650 hammer models and extensive driving system data. Results of the stress computations allow the user to determine whether the pile will be overstressed at a certain penetration or if refusal will likely occur before a desired pile penetration is reached. GRLWEAP also provides an estimate of the static capacity of a pile using the alpha and beta methods. IGM strength values can be input using either SPT N-values, ϕ' , c_u , c_a , or DRIVEN input files.

To determine the geomaterial parameters that have the greatest affect on pile capacity, a parametric study was conducted using the hammer and pile parameters from Bent 1 of MDT Project CN 2144. The pile was a 508 mm closed-end pipe, embedded 5.19 m into a cohesive IGM identified as shale. Additional information on this project is available in Chapter 4 and the appendices. In the parametric study, the percentage change in the final blow count at the CAPWAP capacity was compared to the percent change in the isolated parameter, either quake or damping. A summary of the results are shown in Table 3.1. This study determined that the solution was most sensitive to the damping parameters (toe and shaft). Specifically, of the four dynamic input parameters, toe damping had the greatest affect on the final blow count when compared to toe quake, shaft quake, and shaft damping.

Table 3.1. Parametric Study of GRLWEAP Quake and Damping Parameters

Quake		Damping		Blow Count	% Parameter Change	% BC Change	Ratio: % BC Change/ %Parameter Change
Shaft (mm)	Toe (mm)	Shaft (s/m)	Toe (s/m)				
2.5	2.5	0.65	0.5	87.4			
3	2.5	0.65	0.5	87.6	20.00%	0.23%	1.14%
3.5	2.5	0.65	0.5	87.7	40.00%	0.34%	0.86%
4	2.5	0.65	0.5	87.9	60.00%	0.57%	0.95%
4.5	2.5	0.65	0.5	88	80.00%	0.69%	0.86%
5	2.5	0.65	0.5	88.2	100.00%	0.92%	0.92%
2.5	3	0.65	0.5	89	20.00%	1.83%	9.15%
2.5	3.5	0.65	0.5	90.8	40.00%	3.89%	9.73%
2.5	4	0.65	0.5	92.6	60.00%	5.95%	9.92%
2.5	4.5	0.65	0.5	94.5	80.00%	8.12%	10.15%
2.5	5	0.65	0.5	96.7	100.00%	10.64%	10.64%
2.5	2.5	0.7	0.5	89.1	7.69%	1.95%	25.29%
2.5	2.5	0.8	0.5	92.6	23.08%	5.95%	25.78%
2.5	2.5	0.9	0.5	96	38.46%	9.84%	25.58%
2.5	2.5	1	0.5	99.5	53.85%	13.84%	25.71%
2.5	2.5	1.1	0.5	102	69.23%	16.70%	24.13%
2.5	2.5	1.2	0.5	105.5	84.62%	20.71%	24.47%
2.5	2.5	1.3	0.5	109.1	100.00%	24.83%	24.83%
2.5	2.5	0.65	0.6	94.3	20.00%	7.89%	39.47%
2.5	2.5	0.65	0.7	100.2	40.00%	14.65%	36.61%
2.5	2.5	0.65	0.8	106.7	60.00%	22.08%	36.80%
2.5	2.5	0.65	0.9	113.2	80.00%	29.52%	36.90%
2.5	2.5	0.65	1	119.5	100.00%	36.73%	36.73%

Notes: Input data obtained from MDT Project CN 2144, Bent 1, using *Bearing Capacity – Proportion Shaft Resistance* option in GRLWEAP. BC = hammer blow count.

Existing stresses within the pile during driving also affects the blow count calculations. As a stress wave travels within a pile, the stress may not completely dissipate due to mobilized frictional forces along the pile perimeter. These stresses are known as residual stresses and can affect the calculations (Rausche et al. 2004a). Residual stresses within a pile increase the apparent pile length, which causes higher skin friction and lower tip capacity. Within a standard GRLWEAP analysis, one hammer blow is used to perform the calculation. However, a residual stress analysis requires multiple hammer blows to properly include residual stresses in a drivability analysis

because residual stresses develop over time, increasing with each blow (Briaud and Tucker 1984). Methods are available to perform residual stress analyses, which in the future may provide more accurate results. However, the approach requires extensive calculations that are not well verified at this time. The residual stress approach needs additional testing and refinement before it can be used universally.

3.4 CAPWAP

CAPWAP is a computer program for determining pile resistance based on stress wave calculations using data collected during pile installation. CAPWAP is an acronym for Case Pile Wave Analysis Program. The analysis consists of two parts: 1) field measurements using a Pile Dynamic Analyzer (PDA) and 2) computations using a wave equation model in the CAPWAP software. The PDA includes instrumentation (accelerometers and strain gages) and a closed form solution to the wave equation to provide an approximate prediction of pile resistance during driving. The CAPWAP program improves on computations used in the PDA. CAPWAP uses an iterative solution to the wave equation that varies the quake and damping parameters of the lithology to more accurately determine the capacity. However, the parameter adjustment process is not entirely automated. Certified CAPWAP operators determine the dynamic parameter to adjust in the wave matching process using guidelines provided by Pile Dynamic Inc., the developers of CAPWAP.

The primary advantages of CAPWAP and PDA analyses include:

- reduction or elimination of static load tests,
- assessment of internal pile stresses during driving,
- indication of potential installation problems (if a test pile is used), and
- improved understanding of subsurface conditions and their effect on pile capacities (Baker et al. 1984).

To verify the accuracy of CAPWAP, Likins and Rausche (2004) compiled a database of projects in which both CAPWAP measurements and static load test results were available. This data was examined in detail because the comparisons in the present

study were based solely on CAPWAP results. The authors of this report expanded the Likins and Rausche database through additional literature review.

Using this extensive database, a plot comparing static load test capacities to CAPWAP capacities was assimilated for IGM and soil materials, as shown in Figure 3.2. The plotted data shown in Figure 3.2 indicates there is a strong correlation between CAPWAP and static load testing for both soils and IGMs. This comparison included 115 static load and CAPWAP capacity comparisons; 94 were in soil formations and 21 were conducted in IGM deposits. A table of the references and values used to create this figure are provided in Appendix C.

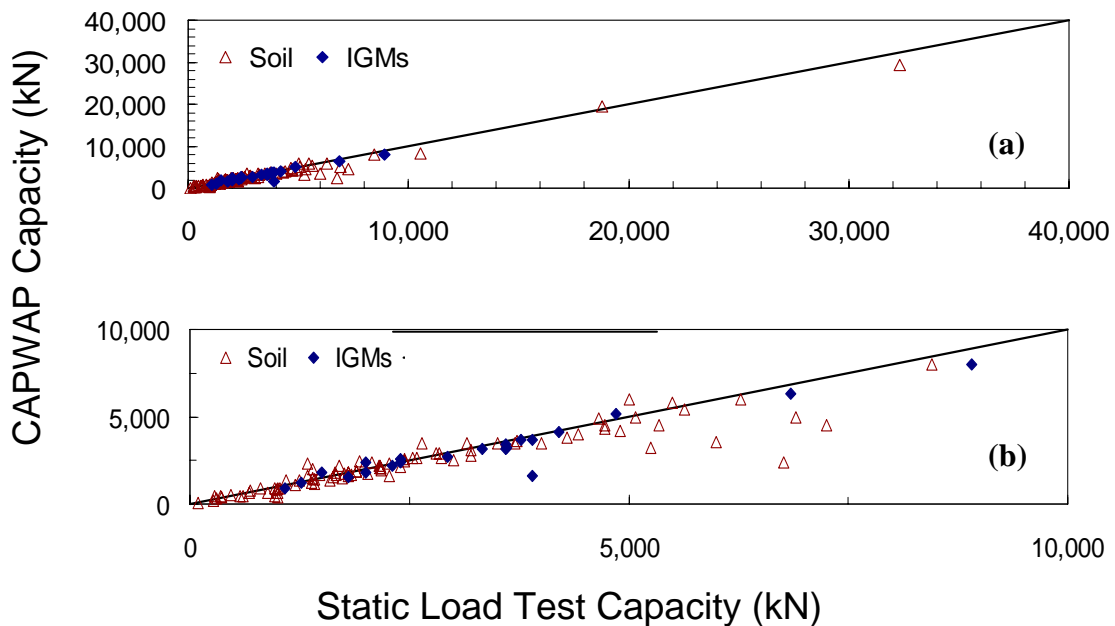


Figure 3.2. Comparison of static load test and CAPWAP capacities from the literature. (a) Full scale plot of all data. (b) Data points at lower capacities.

3.5 Colorado Department of Transportation Method

The Colorado Department of Transportation (CDOT) uses a simplified empirical approach for estimating the capacity of piles driven into IGM formations along the Rocky Mountain Front Range. In the CDOT design method, cohesive IGMs are treated as hard rock. Consequently, the design of piles within these materials relies primarily on the end-bearing capacity, which is assumed to be a function of the structural capacity of the pile material. In this method, the allowable axial resistance of the pile is assumed to be 25% of the pile material yield stress. For example, for a steel pile driven into a cohesive IGM, the allowable design stress will be $0.25f_y$, where f_y is the yield stress of the steel. The allowable capacity is determined by multiplying the allowable design stress by the tip area of the pile.

The depth of driving is estimated based on past experience within the region. Construction specifications require that piles be driven to virtual refusal, which is defined as 2.5 cm or less of penetration for the final 10 blows (CDOT 2005).

4 PROJECT SUMMARIES

The evaluation of piles in IGMs was conducted in this study using data provided by the MDT Geotechnical Section. The data was obtained from bridge projects in which piles were driven into IGM formations and dynamic analyses of pile capacity were conducted. The information provided by MDT contained project specific data from nine bridge construction projects. The following components were analyzed in this study:

- geotechnical design reports,
- boring logs,
- DRIVEN computer analyses,
- project plans,
- contractor hammer submittals,
- dynamic analysis reports, and
- pile driving logs.

The dynamic analyses conducted on each project included PDA and CAPWAP analyses. Pile and geomaterial summaries for each project, organized by MDT control number (CN), are shown in Table 4.1. Further specifics from each project are shown in Table 4.2, including:

- IGM strength (either unconfined compression strength or SPT N-value),
- pile embedment details, and
- IGM stratigraphy in relationship to specific pile locations.

The authors constructed subsurface profiles for each MDT project using the furnished data. The profiles provided in Appendix A graphically show subsurface materials, groundwater table, foundation location, pile embedment, boring locations, and IGM strength measurements from unconfined compression or SPT testing.

Table 4.1. Projects Analyzed in this Study

Project CN	Project Name	Project County	Primary IGM
Q744	Medicine Tree	Lake	Dense Gravel
1744	Vicinity of White Coyote	Lake	Dense Gravel
2144	Nashua Cr.	Valley	Shale
3417	West Fork of Poplar River	Roosevelt	Claystone, Siltstone, Sandstone
4226	Goat Cr.	Lake	Dense Gravel
4230	Bridger Cr.	Gallatin	Dense Gravel
4239	Big Muddy Cr.	Sheridan	Claystone
4244	Keyser Cr.	Stillwater	Dense Gravel

Six of the projects included DRIVEN computer analyses for piles at each of the bridge bents. Projects Q744, 1744 and 4226 were completed before DRIVEN was fully implemented by MDT; consequently, the authors completed DRIVEN analyses for these projects.

A summary of the design and CAPWAP capacities for the piles within the project scope are provided in Table 4.3. The actual (as built) and design (predicted) lengths of the piles are also shown in the table.

On average, cohesive IGMs refused 0.33 m early with a standard deviation of 2.82 m. Cohesionless IGM extended an average of 4.73 m further than planned with a standard deviation of 6.56 m. Thus, on average, the predicted (calculated) resistance of piles in cohesive IGMs was too low, while the calculated resistance of piles in cohesionless IGMs was too high. However, there was considerable variability within each material type, as indicated by the high standard deviation values. For example, within the cohesive IGMs, the error between the calculated design depth and the actual depth required to achieve design capacity varied from 8.61 m greater than the anticipated depth (running) to 3.01 m short of the design depth (early refusal). In Cohesionless IGMs, pile refusal varied from 2.75 m short of the design depth to a colossal 12.17 m greater than the anticipated design depth. Overall, a total sum of 100 m of excess pile

length was required on the nine projects, which amounted to 24.3% of the total pile length that was planned for the projects.

Table 4.2. Project Construction Summaries - IGM Strength

Project CN	IGM Type ⁽¹⁾	Pile Location ⁽²⁾	Pile Type and Size ⁽³⁾	Total Embedded Length (m)	Pile Length in IGM (m)	q _u ⁽⁴⁾ (kN)	SPT N-Value (N ₁) ₆₀ ⁽⁵⁾
Q744	ϕIGM	Bent 1	508mm OP	30.17	15.53	N/A	N _{ref}
		Bent 2	508mm OP	30.11	24.58	N/A	N _{ref}
1744	ϕIGM	Bent 1	H 360x108	21.01	13.71	N/A	N _{ref}
2144	cIGM	Bent 1	508mm CP	27.48	5.19	206 Sh	N/A
		Bent 3	508mm OP	27.58	1.68	83 Sh	N/A
		Overflow 1	508mm OP	25.77	4.77	223 Sh	N/A
3417	cIGM	Bent 1	406mm CP	12.79	9.74	294 C; 40,479 S	N/A
		Bent 2	762mm OP	14.36	8.46	197 C; 367 S	N/A
		Bent 3	762mm OP	14.62	8.52	449 C; 545 S	N/A
		Bent 4	406mm OP	12.80	5.79	579 C; 523 S	N/A
		Overflow 1	406mm OP	15.22	8.52	263 C; 2,808 S	N/A
		Overflow 2	610mm OP	13.62	9.92	328 S; 458 C; 868 C,S,Si	N/A
		Overflow 3	406mm OP	16.2	12.20	709 C; 19,390 S	N/A
4226	ϕIGM	Bent 1	406mm CP	9.3	0.51	N/A	N _{ref}
4230	ϕIGM	Bent 3	610mm OP	8.58	4.58	N/A	N _{ref}
		Bent 4	406mm OP	7.23	3.23	N/A	N _{ref}
4239	cIGM	Bent 1	H 310x125	33.04	4.08	N/A	N/A
		Bent 2	406mm CP	31.14	2.18	N/A	N/A
		Bent 4	H 310x125	41.24	12.28	N/A	N _{ref}
4244	cIGM	Bent 1	H 310x125	9.24	1.92	9,549 Sh; 9,797 S	N/A
		Bent 2	H 310x125	9.21	1.89	N/A	N _{ref}

- 1) cIGM = Cohesive IGM; ϕIGM = Cohesionless IGM; S = Sandstone; Si = Siltstone; C = Claystone; Sh = Shale
- 2) "Overflow" indicates a second overflow structure on the project. The number following Overflow is the bent number of this second structure.
- 3) OP = open-ended pipe pile, CP = closed-ended pipe pile.
- 4) q_u = average unconfined compression strength for the IGM at the Bent.
- 5) N_{ref} = indicates SPT refusal with greater than 50 blows/ 0.3m.

Table 4.3. Project Construction Summaries - Design vs. Actual Construction

Project CN	IGM Type ⁽¹⁾	Pile Location ⁽²⁾	Pile Type and Size ⁽³⁾	Design Axial Capacity (kN)	CAPWAP Measured Axial Capacity ⁽⁴⁾ (kN)	Design Pile Length (m)	Actual Pile Length (m)	Comments
Q744	φIGM	Bent 1	508mm OP	2300	1542, 2308*	18	30.17	Running ⁽⁵⁾
		Bent 2	508mm OP	2300	956, 2140*, 2152**	18	30.11	Running
1744	φIGM	Bent 1	H 360x108	1474	936, 1609*	14.2	21.02	Running
2144	cIGM	Bent 1	508mm CP	2720	2244	29.3	27.48	Early Refusal ⁽⁶⁾
		Bent 3	508mm OP	2825	2388	28.9	27.58	Early Refusal
		Overflow 1	508mm OP	3150	2000, 3160*	26.2	25.77	Early Refusal
3417	cIGM	Bent 1	406mm CP	1810	1800	12.98	12.79	Early Refusal
		Bent 2	762mm OP	3870	3845, 4398*	14.74	14.36	Early Refusal
		Bent 3	762mm OP	3870	3850	14.74	14.62	Early Refusal
		Bent 4	406mm OP	1670	2074	12.97	12.80	Early Refusal
		Overflow 1	406mm OP	1790	2125	16.3	15.22	Early Refusal
		Overflow 2	610mm OP	2870	3074, 4294*	15.83	13.62	Early Refusal
		Overflow 3	406mm OP	1560	2598	17.03	16.2	Early Refusal
4226	φIGM	Bent 1	406mm CP	1950	1649	12.05	9.3	Early Refusal
4230	φIGM	Bent 3	610mm OP	2600	3200	8.58	8.58	
		Bent 4	406mm OP	2430	3195	7.23	7.23	
4239	cIGM	Bent 1	H 310x125	2025	2125	30.54	33.04	Running
		Bent 2	406mm CP	2205	2370	32.64	31.14	Early Refusal
		Bent 4	H 310x125	2025	2202	32.64	41.24	Running
4244	cIGM	Bent 1	H 310x125	2230	3500	12.22	9.24	Early Refusal
		Bent 2	H 310x125	2230	2550	12.22	9.21	Early Refusal

- 1) cIGM = Cohesive IGM, φIGM = Cohesionless IGM
- 2) “Overflow” indicates a second overflow structure on the project. The number following Overflow is the bent number of this second structure.
- 3) OP = open-ended pipe pile, CP = closed-ended pipe pile.
- 4) “*” indicates restrrike capacity. “**” indicates a second restrrike capacity.
- 5) “Running” indicates the pile required driving further than the design embedment in order to achieve the required capacity.
- 6) “Early Refusal” indicates that the pile could not be driven to the design embedment without probable structural damage.

Piles driven at very high blow counts (small set) into stiff materials are prone to structural damage from excessively high stresses. As an independent check of potential pile damage, the maximum driving stresses for the piles in each project were compiled and compared with allowable driving stresses based on AASHTO (1996) bridge specifications. Data for this comparison was compiled using information obtained from the CAPWAP analysis reports. The motivation behind the evaluation was the premise that pile damage during driving may partially explain the wide variability between predicted and actual capacities. As shown in Table 4.4, relatively high stresses occurred during pile driving in all the projects analyzed. The higher stressed piles (i.e., piles that experienced stresses in excess of 90% of the allowable driving stress) were driven into both cohesive and cohesionless IGMs; that is, there were no discernable trends based on IGM type. Of the higher stressed piles, 30% exceeded the allowable driving stress recommended by AASHTO (1996). The piles were all steel pipe piles driven (open or closed ended).

Table 4.4. Computed Stresses within Piles During Driving

CN	Bent ¹	IGM Type	Pile Size and Type ²	f_y^3 (MPa)	Allowable Driving Stresses (MPa)	Maximum Compressive Stresses (MPa)	% of Allowable Driving Stress
3417	O1	CH	P406	310	279	286.2	102.6%
3417	O3	CH	P406	310	279	282.9	101.4%
4239	2	CL	P406	241	216.9	219.9	101.4%
3417	1	CH	P406	310	279	276.5	99.1%
Q744	1R	CL	P508	310	279	207	74.2%
3417	4	CH	P406	310	279	261.8	93.8%
Q744	2RR	CL	P508	310	216.9	201.2	72.1%
Q744	2R	CL	P508	310	216.9	200.4	71.8%
Q744	2	CL	P508	310	216.9	198.1	71.0%
2144	O1R	CH	P508	310	279	251.6	90.2%

Notes:

- 1) “R” indicates values from a CAPWAP restrrike analysis, and “RR” indicates values from a second CAPWAP restrrike analysis.
- 2) “P” indicates pipe pile, and the number following is the pile diameter in mm.
- 3) f_y is the yield stress of the steel.

Although driving stresses were relatively high, there was no indication in any of the CAPWAP reports that pile damage occurred or was suspected. The authors recommend that during design, careful consideration be given to evaluating pile stresses and potential pile damage if IGM formations are expected at the site. It may be prudent to use a range of IGM strength parameters (parametric study) in this evaluation because of the variable nature of these materials and the real potential for excessively strong and excessively weak anomalies within the IGM deposit.

5 ANALYSIS OF PROJECT DATA

For the analyses conducted in this study, IGMs were divided into two broad categories, cohesive and cohesionless. Cohesive IGMs have an intrinsic bonding or cohesion within their structure; for example, claystone, sandstone and siltstone. Cohesionless IGMs are very dense materials, often sandy gravels, which do not contain any bonding between the particulates.

Data analyzed in this study were compiled from information provided by MDT, as described in previous chapters. Information from each of the nine projects was collected and compiled, including initial drive and restrike data. CAPWAP information was obtained from reports completed for each project. Unless noted otherwise, DRIVEN inputs for each bent were obtained from the DRIVEN reports provided by MDT. GRLWEAP analyses were conducted by the author for each project bent using hammer and cushion information submitted by the contractor. Remaining information was determined using engineering judgment based on the soil profiles and foundation reports. A spreadsheet containing all of the above information was compiled and is provided in Appendix B.

The methodology behind this research is iterative. Evaluations were conducted by creating numerous parametric comparisons to search for trends or useful relationships within the available information. The variability of IGM materials provided an interesting challenge because of the unpredictable response of the material to pile driving and because of the many variables involved with pile driving and pile resistance. The analytical comparison was divided into the following three phases:

- 1) evaluate the accuracy of current design procedures,
- 2) investigate possible correlations between project data and predictive methods, and
- 3) determine the accuracy of other capacity prediction methods.

The following subsections describe the evaluations and comparisons in terms of these broadly defined phases.

5.1 Evaluate Accuracy of Current Design Procedures

The first step within the analysis was to determine the accuracy of the current design methods used by many designers, including the MDT Geotechnical Section. This evaluation was conducted by comparing the calculated static capacities (using the program DRIVEN) to measured dynamic capacities from CAPWAP. The DRIVEN capacities used in this comparison were created using parameters determined from the DRIVEN reports provided by MDT, or if none were available, the authors created input files based on properties determined from information that was provided in the geotechnical project report. The depths used to determine capacities were obtained directly from the CAPWAP reports. End-of-driving depths were used for the capacity calculations on all projects. If a restrike CAPWAP analysis was conducted, the embedment depth at the end of restrike was used to determine the restrike capacity.

A comparison of the capacity values is shown in Figure 5.1. Shaft and toe capacity comparisons are provided in Figure 5.2 and Figure 5.3, respectively. The ordinate of these plots represents the calculated capacities using original input parameters. The abscissa represents the measured dynamic capacities from the CAPWAP analyses, for initial drive and restrike. The diagonal 45° line in each plot can be used to visually assess the accuracy of calculated predictions using the DRIVEN program with original, unaltered parameters.

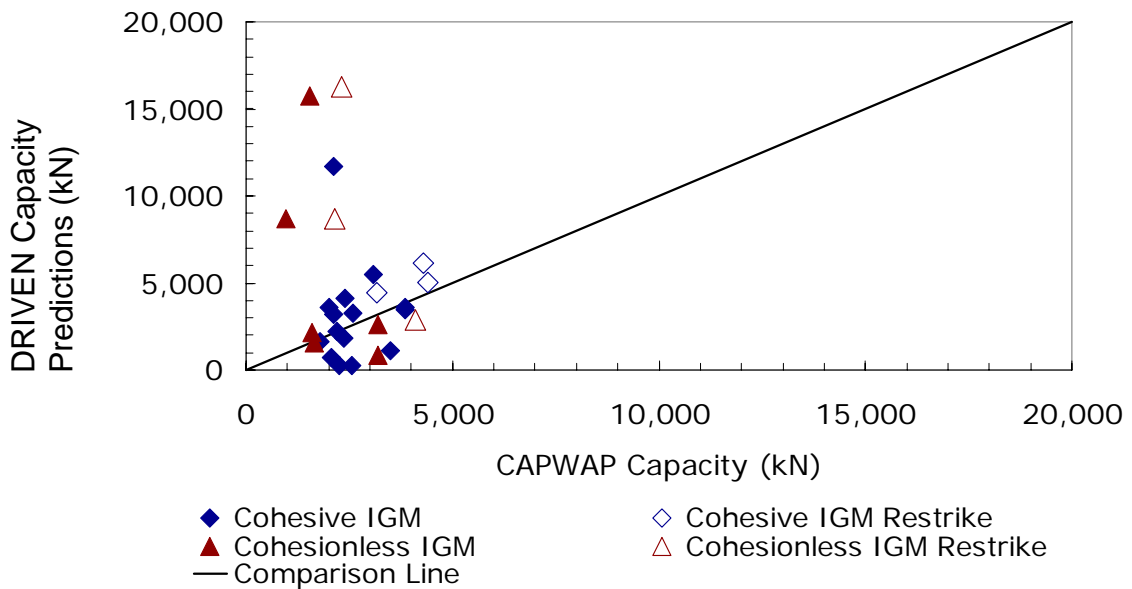


Figure 5.1. Comparison of predicted total capacity to measured CAPWAP capacity.

The capacity comparisons shown in Figure 5.1 clearly demonstrate the inherent variability of pile resistance in IGMs. Most of the projects exhibited considerable variation between predicted capacities calculated using DRIVEN and the measured CAPWAP capacity. For example, five of the six restrike analyses were over predicted using DRIVEN, one by as much as 580% (a factor of 6.8).

To further refine the analyses, the data was further dissected into shaft and toe resistances. As shown in Figure 5.2, the shaft resistance was under predicted in 12 out of 20 (60%) occurrences in cohesive IGMs; however, there were outliers in which capacity was over predicted by 150% to 380%. The majority of shaft capacity predictions for cohesionless IGMs were less than the measured CAPWAP capacities; the worst case was a 400% under prediction (a factor of 5). Toe capacity predictions were also quite variable and random, as shown in Figure 5.3, with no discernable trends.

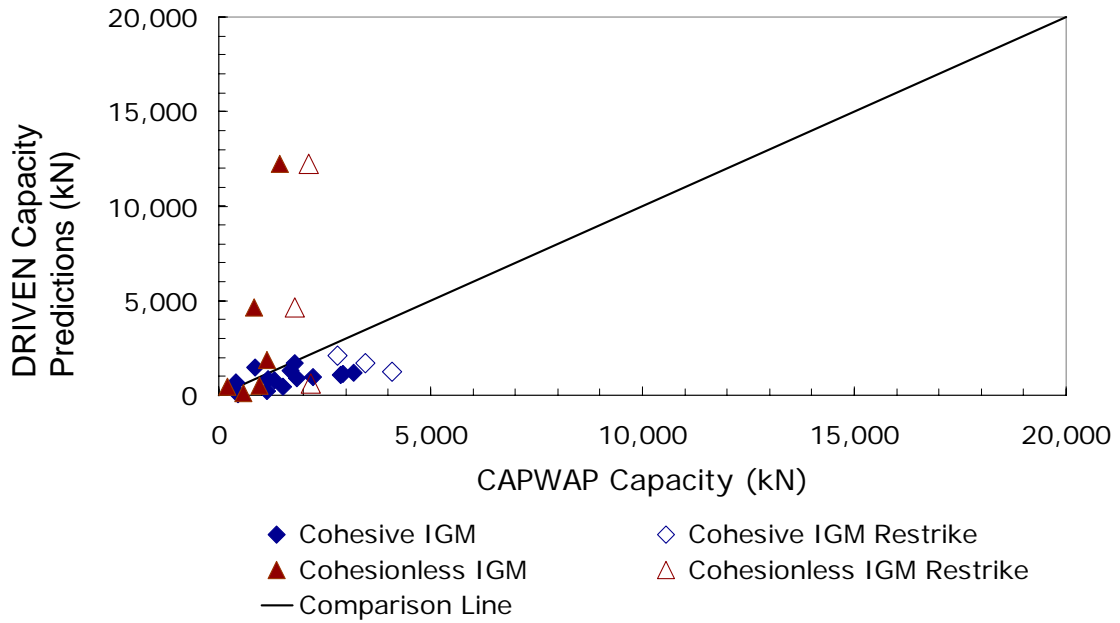


Figure 5.2. Comparison of predicted shaft capacity to measured CAPWAP shaft capacity.

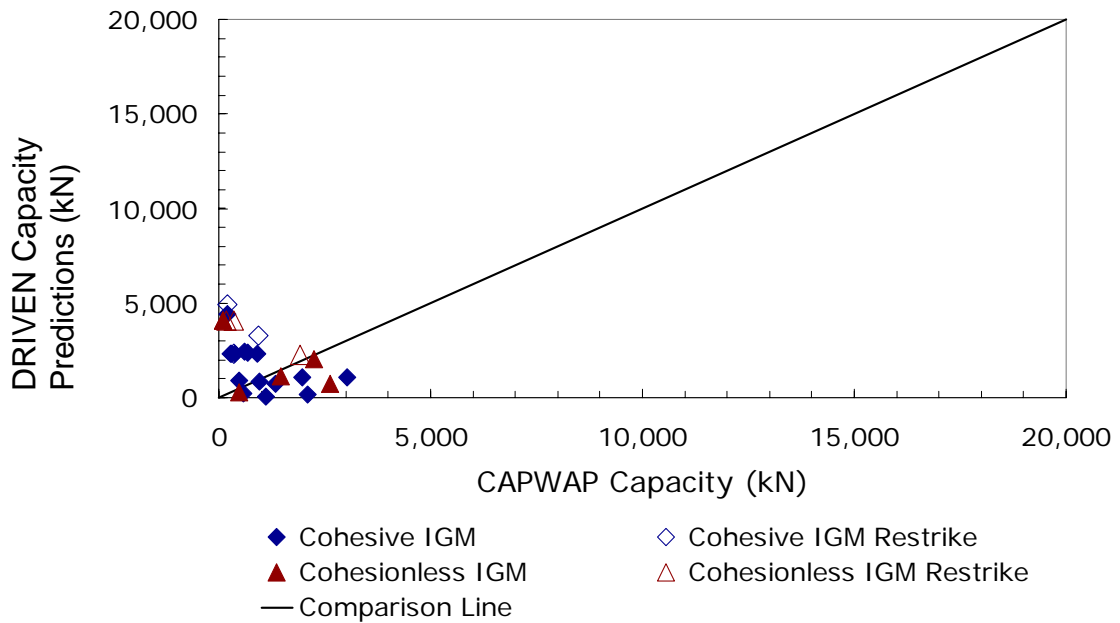


Figure 5.3. Comparison of predicted toe capacity to measured CAPWAP toe capacity.

The comparisons shown in Figures 5.1, 5.2, and 5.3 were made using the original DRIVEN computer files and soil parameters, with no after-the-fact modifications. This is similar to a class A prediction and indicates that semiempirical methods developed for soil may yield unreliable predictions for piles driven into IGM deposits. The computed results may have little to no correlation with the CAPWAP capacity measured during pile installation.

The following sections describe results of additional data analyses that were conducted to search for trends or correlations that could be used to improve calculated predictions through modification of IGM input parameters or analytical methods.

5.2 Investigation of Possible Correlations

More detailed analyses of both shaft and toe capacity were conducted to examine the data for potential trends or correlations using two approaches: 1) normalized capacity comparisons and 2) iterative solutions. The normalized capacity comparisons included CAPWAP resistances normalized by pile geometry. The iterative solutions were developed by varying IGM strength parameters until computed capacities matched measured CAPWAP capacities.

5.2.1 Normalized Capacity Comparisons

Normalized capacity comparisons allow potentially more accurate comparisons of data between projects by isolating material properties from measured values. The pile perimeter, the pile toe area, and the length of the pile within the IGM were used to normalize the CAPWAP shaft and toe capacities. The normalized shaft resistance was defined using the following equation:

$$N_{shaft} = \frac{CAPWAP_{shaft}}{p} \quad (2)$$

where, N_{shaft} is the normalized shaft resistance, p is the perimeter of the pile and $CAPWAP_{shaft}$ is the measured CAPWAP shaft resistance.

The normalized toe resistance was determined using the following equation:

$$N_t = \frac{CAPWAP_{toe}}{A} \quad (3)$$

where, N_t is the normalized toe resistance, A is the plugged area of the pile, and $CAPWAP_{toe}$ is the measured toe resistance. The plugged area is the full toe area of the pile; a box area for H-piles and the entire circular area for pipe piles.

The length of pile within IGM layer is compared to N_{shaft} in Figure 5.4. There is potentially a slight trend within the data, which consists of a weak linear relationship from coordinate points (0, 0) to (7, 1,500). The data trends downward and shows considerable scatter beyond this point.

The CAPWAP shaft capacity included within this calculation is the total shaft capacity of the pile; unfortunately, this also includes the shaft resistance from the soil layers above the IGM deposit. For the projects evaluated in this study, the shaft capacity in the upper soil layers was not measured during pile driving, and predicted values of shaft capacity involve a high degree of uncertainty and are thus too unreliable to use as a refinement to the measured values. The authors believe the trend or correlation could be improved if the soil and IGM shaft resistances were separated from the total CAPWAP shaft resistance.

It is in the nature of IGMs to vary with geology, location, and depth. For this reason, the normalized shaft resistance comparison was also analyzed by project. As shown in Figure 5.5, there is some clustering of data points by project. The most varied projects are those with cohesionless IGMs; specifically, project numbers 4239 and Q744. The projects with piles in cohesive IGMs show trends of weakly-defined clusters; for example, project numbers 2144, 3417 and 4244.

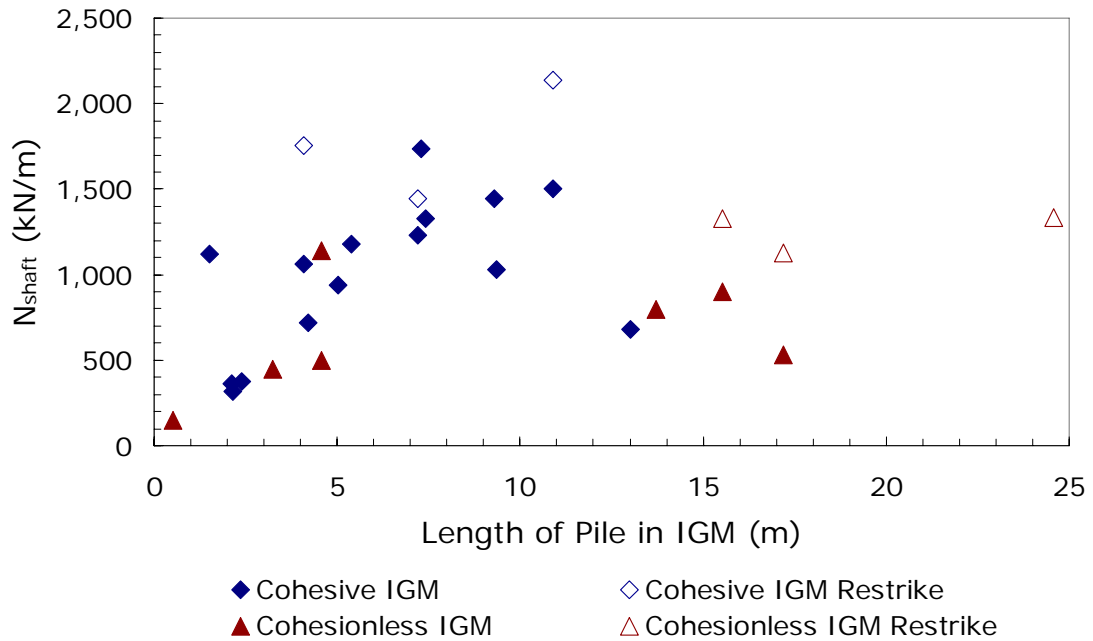
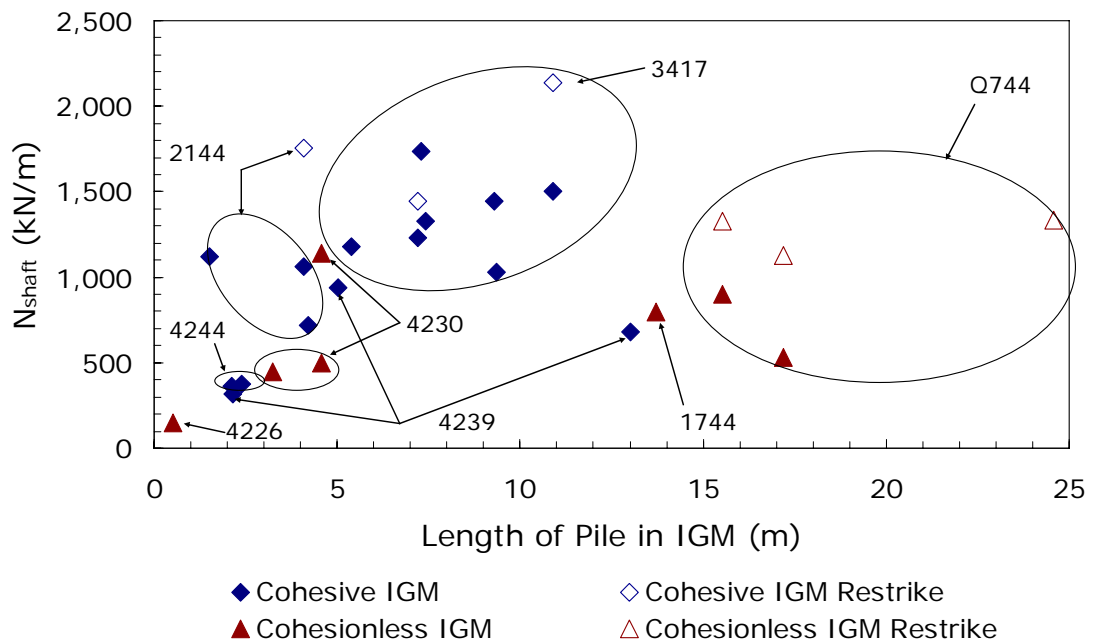


Figure 5.4. Normalized shaft resistance compared to pile length in IGM.



Note: Four digit numbers are MDT project control numbers.

Figure 5.5. Normalized shaft resistance with project number designation.

Normalized toe capacity (N_t) was compared with unconfined compression strength (Figure 5.6) and with pile length in IGM (Figure 5.7). As shown in Figure 5.6, the comparison of toe capacity with unconfined compression strength indicates large data scatter with no apparent trend. Intuitively, an increase in toe capacity would be expected to occur as the unconfined compression strength of the IGM increases; however, this was not the case for the data evaluated. These uncharacteristic results may be attributed to changes in material properties during pile driving. Post installation material properties of the IGM are not accurately known because the pile driving process can result in significant alterations of the material.

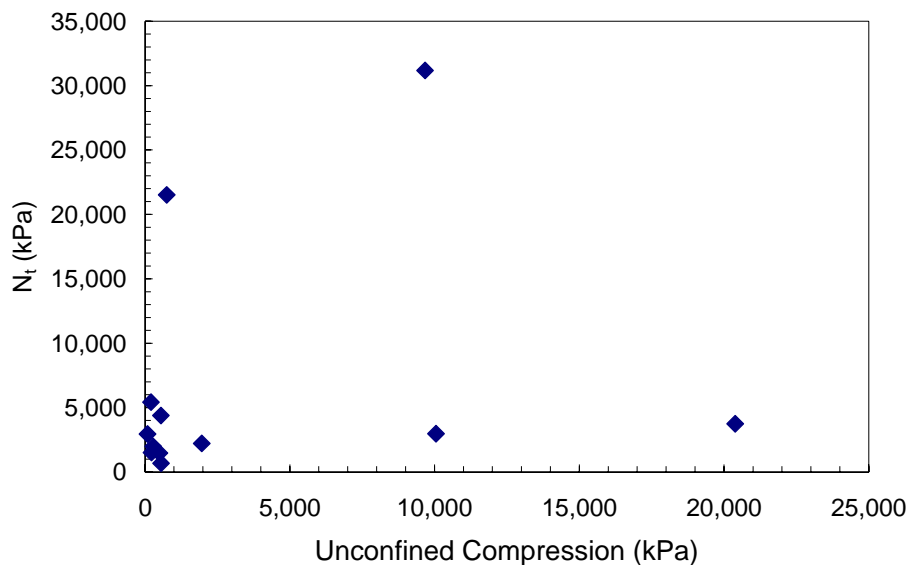


Figure 5.6. Comparison of normalized toe resistance with unconfined compression strength of cohesive IGMs.

Figure 5.7 shows a slight correlation of decreasing toe capacity with the length of pile driven into the IGM layer. However, because of changes in material properties during pile driving and geologic trends in which the IGM strength changes with depth, the correlation is limited in its usefulness.

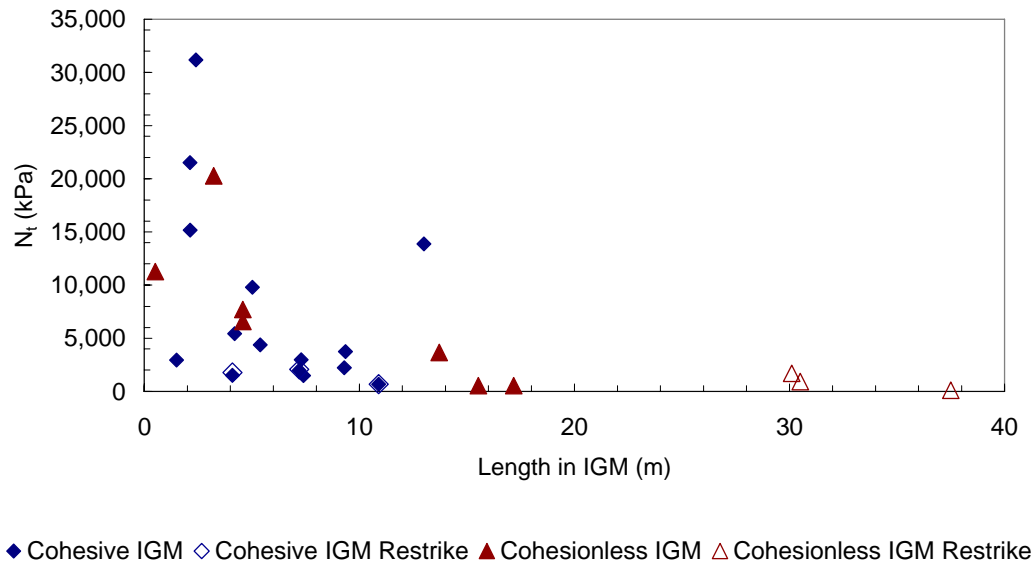


Figure 5.7. Comparison of normalized toe resistance with length of pile in IGM.

5.2.2 Iterative Solutions

Iterative solutions were created by varying material parameter input values until the DRIVEN predicted capacity matched the CAPWAP total resistance and shaft resistance. The following equation was used to vary the inputs in each IGM layer:

$$Input_{new} = M \times MDT_{input} \quad (4)$$

where, $Input_{new}$ is the new revised variable, M is the strength multiplier, and MDT_{input} is the original input used in the MDT report. MDT_{input} included only the strength parameters for the IGM layers, which were undrained cohesion for cohesive IGMs and ϕ' for cohesionless IGMs. The multiplier M was varied until $Input_{new}$ resulted in a calculated capacity that matched the measured CAPWAP capacity at the final constructed field depth, to within $\pm 1.0\%$. This process was used to match the capacity from both initial drive and restrike CAPWAP analyses.

Most of the projects did not require considerable variation to match the CAPWAP capacities. Figure 5.8 shows the number of M values (ordinate) within a certain range (abscissa). Seventy percent of the M values were within the range of 0.9 to 1.1. This

indicates that relatively small changes to the input strength parameters can result in relatively large changes in computed capacities. Nine of the 28 CAPWAP analyses were excluded from this comparison because the IGM strength inputs could not be reasonably altered to match the ultimate CAPWAP capacity. For example, projects with cohesionless IGMs were excluded in this comparison when the multiplier resulted in a friction angle of 50° or greater.

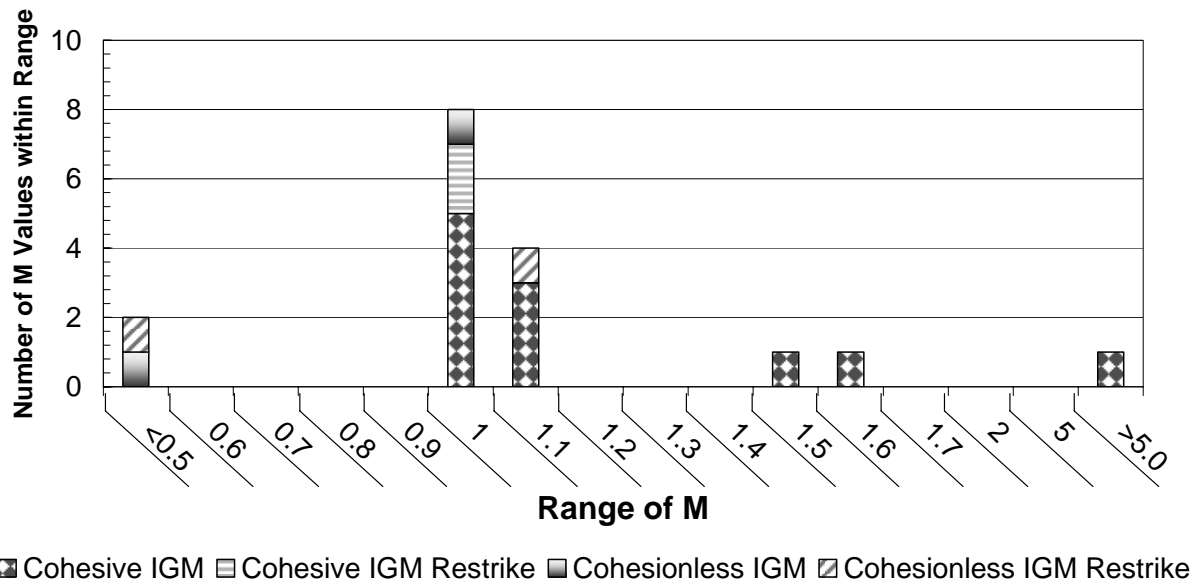


Figure 5.8. Strength multiplier use to match measured CAPWAP capacities.

It was hypothesized that M might correlate with either the pile length in IGM layer, or the CAPWAP capacity. Using the M -multiplier concept, a comparison was made with the pile length in IGM layer and the measured CAPWAP capacity, as shown in Figure 5.9 and Figure 5.10, respectively. The M value was plotted on a logarithmic scale to better distinguish the data points. The cluster of M values near 1.0 is apparent in these comparisons, indicating that only modest changes to input parameters are required to match field capacities. However, because of the significant scatter and the lack of any logical trends, it is concluded that the M values do not depend solely on the pile length in

IGM or the measured CAPWAP capacity. This further confirms previous comparisons described in this chapter.

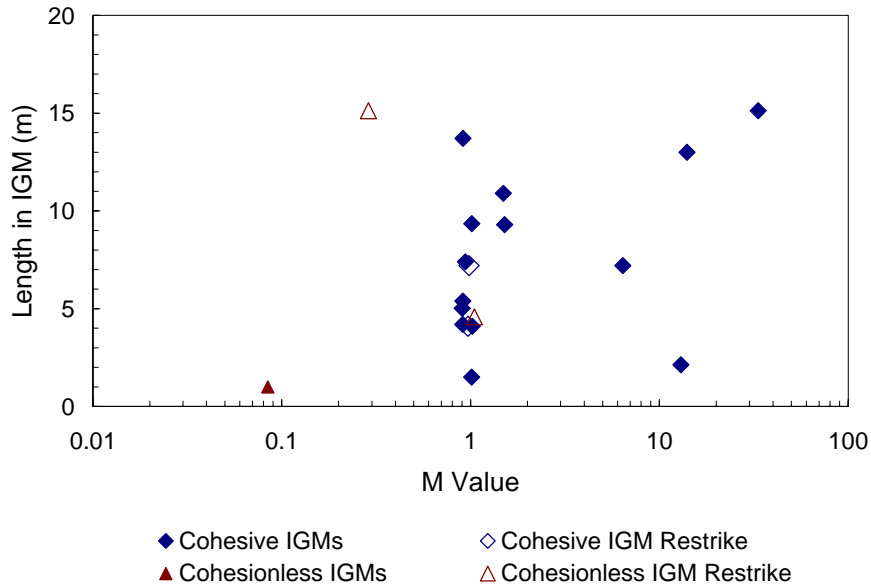


Figure 5.9. Comparison of M required for a CAPWAP capacity match to the pile length in IGMs.

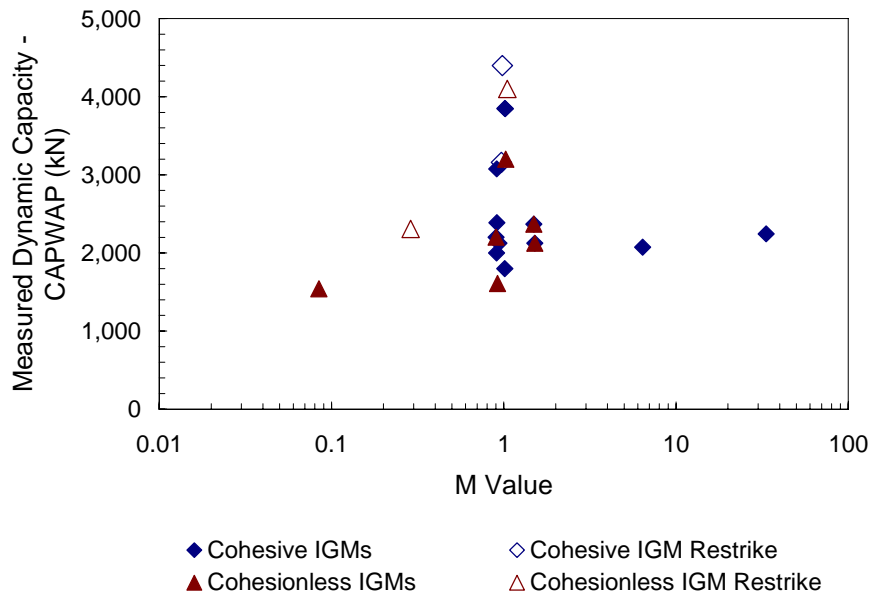


Figure 5.10. Comparison of M required for a CAPWAP capacity match to the measured CAPWAP capacity.

Numerous additional comparisons were examined using this iterative approach. These comparisons were generally unsuccessful at producing useful correlations or trends that could be used to improve design approaches. This further supports previous observations regarding the highly variable and heterogeneous nature of IGM deposits.

5.3 Accuracy of Other Capacity Prediction Methods

This subsection summarizes an evaluation of three alternate approaches for predicting axial capacity using the project data provided by MDT. The methods evaluated included the FHWA Gates dynamic formula, the WSDOT dynamic formula, and a method used by the Colorado Department of Transportation, herein called the CDOT method.

The following version of the Gates dynamic formula was used in this analysis:

$$R_{Gates} = 1.75\sqrt{1,000 \times E^* \log_{10}(10N_c)} - 100 \quad (5)$$

where, R_{Gates} is the pile axial capacity, E^* is the energy of the hammer in foot-pounds, and N_c is the pile penetration resistance in blows per inch.

The WSDOT Gates Driving Formula represents the newest addition to the exhaustive collection of pile dynamic formulas. Allen (2007) used a large database of pile driving information to calibrate and modify the Gates dynamic formula to provide more accurate solutions for conditions encountered on transportation projects in the state of Washington. The database contained information from pile static load tests, end-of-driving blow counts, and beginning of restrike blow counts. Using information provided in the MDT project CAPWAP reports, pile capacities were calculated using the WSDOT Gates formula using two approaches based on the source of hammer energy values: 1) measured hammer energy (R_{WA1}), and 2) predicted hammer energy (R_{WA2}).

Approach 1 uses the predicted or assumed hammer energy as follows:

$$R_{WA1} = 6.6 \times F_{eff} \times E^* \times \ln(10N_c) \quad (6)$$

where, R_{WA1} is the pile axial capacity based on predicted hammer energies, F_{eff} is an efficiency factor for specific hammers and pile types, E^* is the energy of the hammer in foot-pounds, and N_c is the pile penetration resistance in blows per inch. Hammers on all

of the MDT projects were open-ended diesel hammers on steel piles; thus, based on recommendations by Allen (2007), F_{eff} is 0.47. E^* in this case represents the potential energy of the hammer, or the stroke of the hammer multiplied by the ram weight. The penetration resistance, N_c , was obtained directly from the CAPWAP reports provided by MDT.

Approach 2 uses the measured hammer energy as follows:

$$R_{WA2} = 6.6 \times TE \times \ln(10N_c) \tag{7}$$

where, R_{WA2} is the pile axial capacity based on measured hammer energies, and TE is the energy transferred to the pile as measured by gauges attached to the pile during dynamic testing. TE values were directly input into the equation without any adjustment for hammer efficiency because this value was directly measured during pile driving. A comparison of the WSDOT Gates formulas utilizing measured and predicted energies are compared to CAPWAP capacities in Figure 5.11.

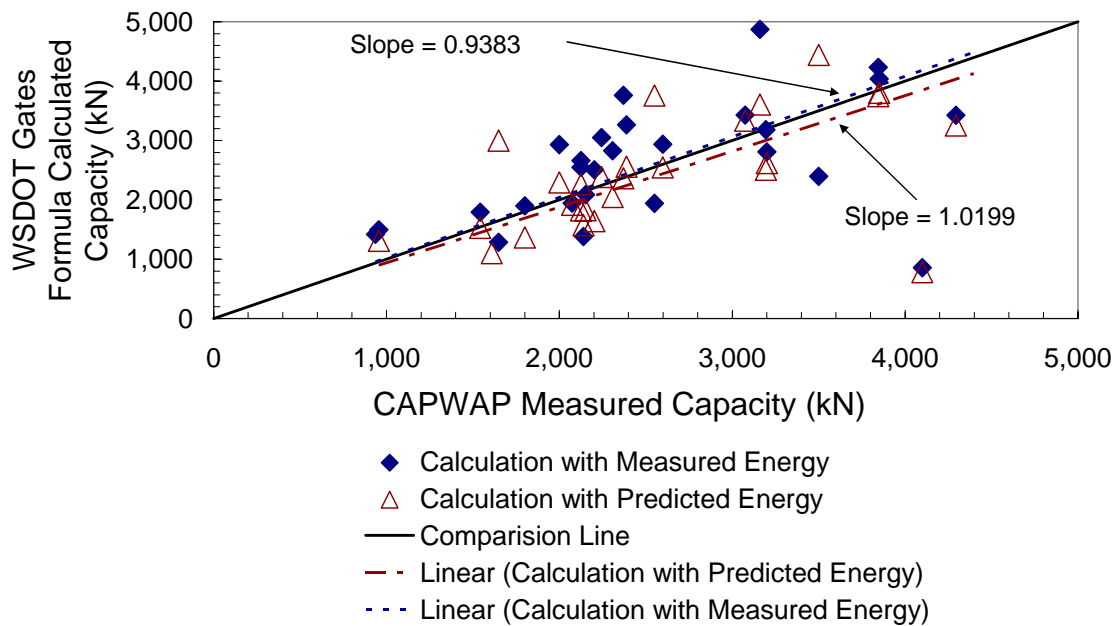


Figure 5.11. Comparison of the calculated WSDOT Gates capacities to the measured CAPWAP capacity.

As shown in Figure 5.11, relatively good matches between predicted and measured CAPWAP capacities were obtained from both forms of the WSDOT Gates formula. Capacity determinations using the measured hammer energy (R_{WA2}) provided a slightly better match; however, the difference in results between the equations was relatively insignificant.

Pile axial capacity can be estimated using the CDOT method with the following equation:

$$R_{CDOT} = 0.25 \times f_y \times A_{open} \times FS \quad (8)$$

where, R_{CDOT} is the pile axial capacity, f_y is the yield stress of the steel, A_{open} is the cross sectional area of the pile, and FS is the factor of safety used in design (FS = 3).

Comparisons of capacities calculated using the FHWA Gates dynamic formula, the WSDOT dynamic formula, the CDOT method, and the DRIVEN and GRLWEAP computer programs are shown in Figure 5.12 and Figure 5.13 for cohesive and cohesionless IGMs, respectively. Calculated capacities are compared to measured CAPWAP capacities using original unmodified input values obtained from the MDT project reports. Figure 5.12(a) shows all of the data, while Figure 5.12(b) shows more detail for the lower capacity values. Capacities calculated using the CDOT method and the FHWA Gates dynamic formula consistently under predicted the measured capacities by relatively large amounts. The predicted capacities determined from DRIVEN and GRLWEAP were in relatively good agreement; however, neither accurately matched the measured CAPWAP capacity. Overall, the WSDOT Gates formula provided the best match to the measured CAPWAP capacities.

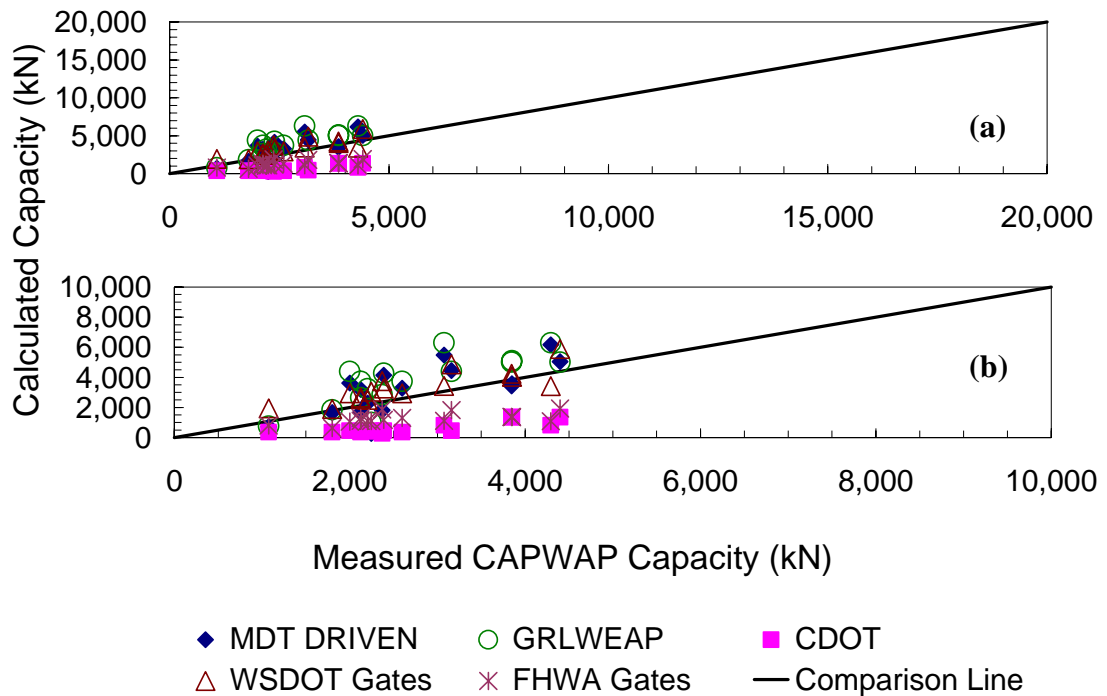


Figure 5.12. Comparison of capacity calculations in cohesive IGMs. (a) Full scale. (b) Detail at lower capacities.

Comparisons of predicted capacities are shown in terms of project bents for cohesive IGMs (Figure 5.14) and cohesionless IGMs (Figure 5.15). Analytical predictions for piles in cohesionless IGMs (shown in Figure 5.15) exhibited even greater scatter than the cohesive IGM projects (shown in Figure 5.14). Overall, the previous trends described for the cohesive IGM predictions apply equally to the cohesionless IGM predictions. That is, the FHWA Gates, CDOT, DRIVEN, and GRLWEAP predictions were relatively poor, while the WSDOT Gates formula provided the most accurate predictions of the measured CAPWAP capacities.

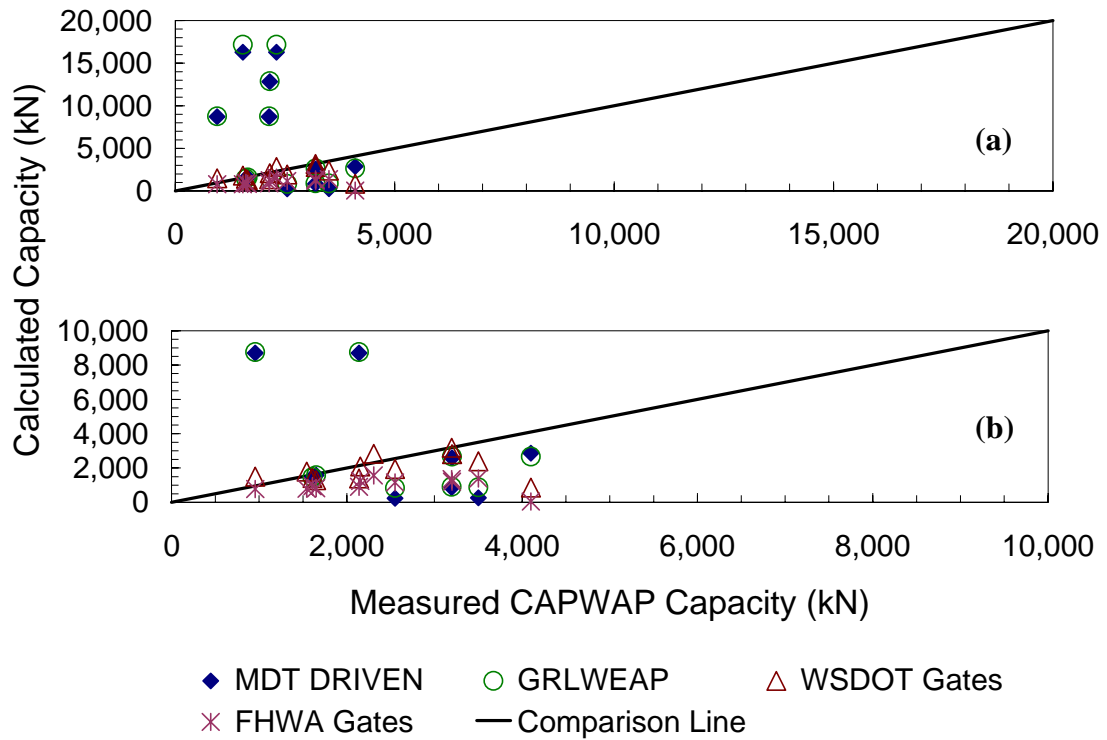


Figure 5.13. Comparison of capacity calculations in cohesionless IGMs. (a) Full scale. (b) Detail of points at lower capacities.

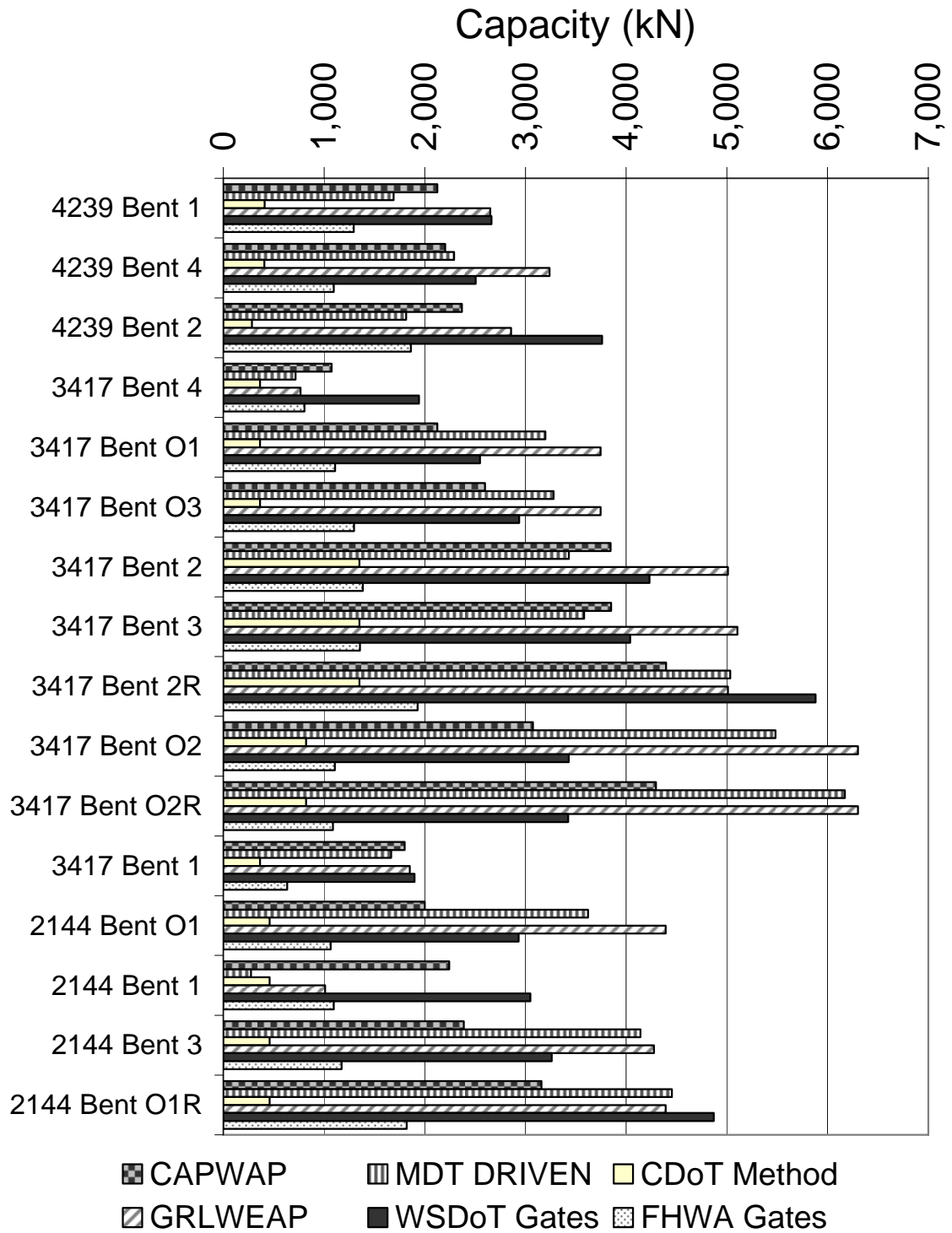


Figure 5.14. Comparison of capacity calculations in cohesive IGMs compared by project number and bent.

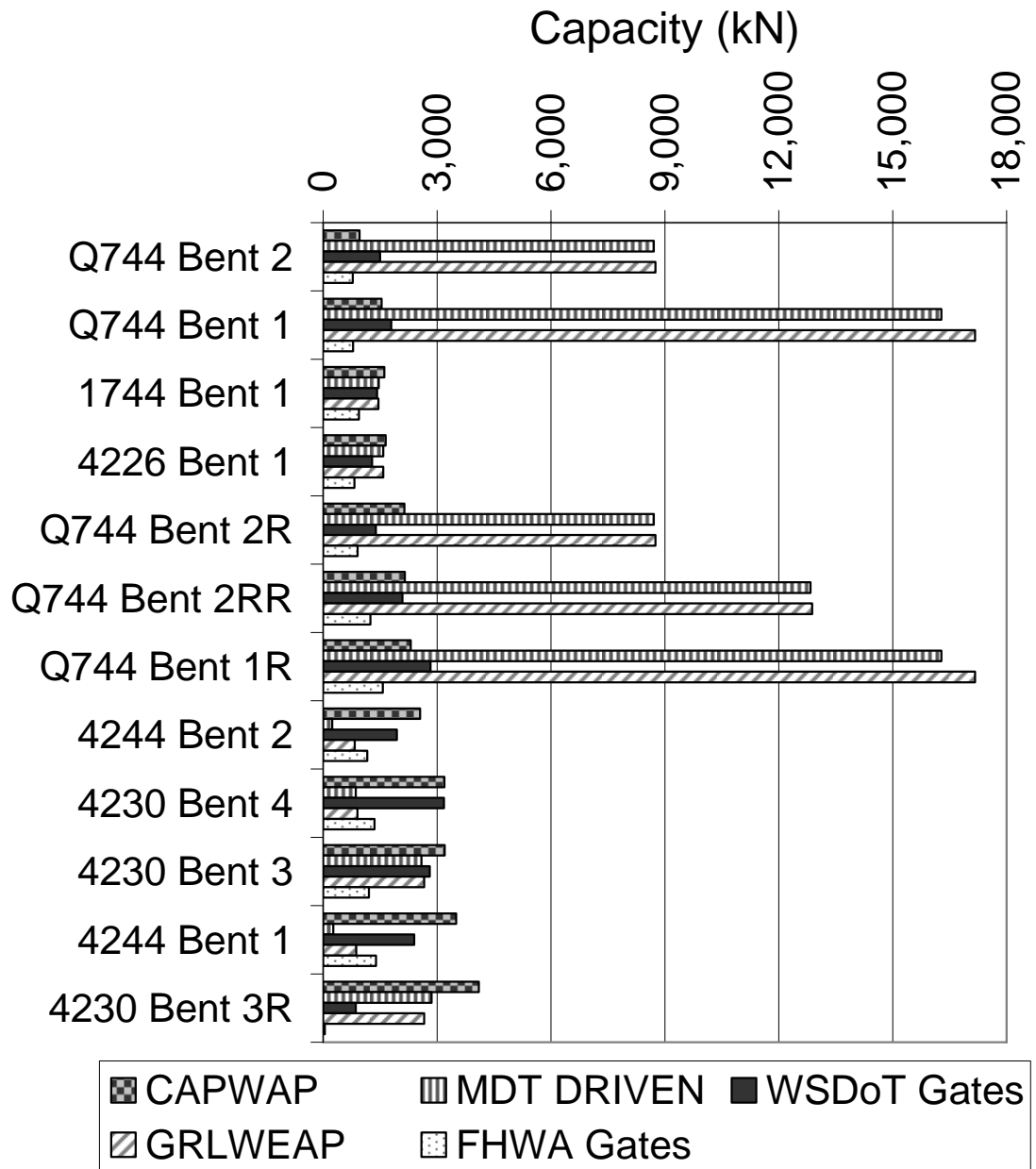


Figure 5.15. Comparison of capacity calculations in cohesionless IGMs compared by project bent.

In summary, a static load test represents the most accurate method for determining the axial capacity of a pile driven into an IGM deposit. However, the expense of a static load test is not justified on all projects. In these cases, PDA measurements with CAPWAP analyses provide the next most reliable option at a lower cost. Based on the data analyzed in this the study, it appears that the WSDOT Gates formula may be the best alternative to use as a check of CAPWAP results or as an approximate estimate of capacity during pile driving.

6 SUMMARY AND CONCLUSIONS

Construction experience with piles driven into IGM deposits indicates the predicted behavior frequently does not match the field pile response. Piles either refuse early or drive further than anticipated. This report summarizes the results of analyses conducted on project data from nine Montana bridge projects in which steel piles were driven into a variety of different IGM deposits. The project data were analyzed to discern trends or correlations that could be used to improve the reliability of pile capacity predictions in different IGM formations.

An overview of IGMs including material behavior, sampling and testing methods, axial capacity design methods, and experiences with foundations founded in IGMs was provided based on information compiled and synthesized from a thorough literature review. In summary, there are two broad categories of IGMs: 1) cohesive and 2) cohesionless. Cohesive IGMs have an intrinsic bonding and include fine-grained materials such as mudstone, claystone, siltstone and sandstone. Cohesive IGMs are typically identified as materials with unconfined compressive strengths between 0.5 to 25 MPa. Cohesionless IGMs do not have any apparent bonding between the particulates of the material and generally consist of very dense sandy gravel deposits with varied amounts of silt. SPT N-values greater than 50 blows per 0.3 meters define a cohesionless IGM.

The material behavior of IGMs should be considered from geological and geotechnical perspectives when conducting foundation analyses. The geological study provides information regarding formation properties, type of bonding, and regional heterogeneity that may be expected within the formation. The geotechnical study provides information regarding material properties, strength as a function of stress state, compressibility and stiffness characteristics, and pore pressure characteristics.

Sampling and testing difficulties represent the largest hurdle that must be overcome to improve our understanding of IGM behavior and to improve the methods for predicting the response of structures founded in IGMs. Accurate material properties cannot be determined unless quality samples are obtained from the field. Rock coring

and SPT sampling methods are not adequate for obtaining quality undisturbed samples of IGMs. In-situ test methods, such as the pressuremeter, provide the most promise for determining accurate strength and stiffness parameters in IGMs. However, advanced in-situ methods can be expensive and may require further refinement and development before they can be practically implemented on a routine basis.

Deep foundation experience with IGMs has predominantly focused on drilled shafts. Based on documented experience in the literature, the installation method and its affect on the IGM material property was found to govern the drilled shaft capacity. The literature contains very limited practical or applied information regarding piles driven into IGM formations. The majority of previous studies are site or project specific, and somewhat inconsistent in regards to observations and results. Similar to drilled shafts, the overriding issue with driven piles pertains to proper characterization of the IGM properties (primarily strength and compressibility). Proper characterization of material properties is no simple task; and to date, is not adequately conducted on most projects because of the difficulties in sampling and testing IGMs, and because of the unknown changes that occur in the IGM deposit during pile driving.

Computerized analytical tools typically used for pile design include DRIVEN, GRLWEAP and CAPWAP. DRIVEN uses inputs of site conditions, soil strength properties, and pile properties to determine the pile capacity. GRLWEAP is used to calculated capacity and to assess the pile driving hammer system and the pile drivability. Calculations in GRLWEAP are based on stress-wave theory. DRIVEN and GRLWEAP have a long history of use and work well for piles driven into most types of soils. One of the goals of this study was to investigate the suitability of these programs as design tools for piles driven into IGMs. Two additional pile driving formula were evaluated: the FHWA Gates formula and the WSDOT Gates formula.

CAPWAP is a capacity determination tool that uses data measured during pile driving in conjunction with a wave equation analysis to determine the capacity of pile foundations. Case studies in which a CAPWAP analysis and a static load test were conducted on the same project were compiled into a database. From this information, it was determined that the CAPWAP dynamic capacity is well correlated to the static load

test capacity. Due to the high accuracy of the CAPWAP capacities when compared to static load tests, the CAPWAP capacity was used as a baseline comparison in this study.

The capacity comparisons evaluated using measured data from nine Montana bridge projects clearly demonstrated the inherent variability of pile resistance in IGMs. Results from the majority of the projects exhibited considerable variation between predicted capacities calculated using DRIVEN and measured CAPWAP capacities. For example, five of the six restrike analyses were over predicted using DRIVEN, one by as much as 580%. In these projects, the shaft resistance was under predicted in 12 out of 20 (60%) occurrences in cohesive IGMs; however, there were outliers in which capacity was over predicted by 150% to 380%. The majority of shaft capacity predictions for cohesionless IGMs were less than the measured CAPWAP capacities; the worse case was a 400% under prediction (a factor of 5). Toe capacity predictions were also quite variable and random, with no discernable trends.

The predicted capacities determined from DRIVEN and GRLWEAP were in relatively good agreement; however, neither accurately matched the measured CAPWAP capacities. Overall, for the data evaluated in this study, the WSDOT Gates dynamic formula provided the best match to measured CAPWAP capacities.

Comparisons of data from nine projects provided by MDT were not conclusive enough to derive a more accurate capacity prediction method for future use. The WSDOT Gates driving formula shows promise as a good approach for checking capacity during pile installation, when dynamic testing is not economical. The CDOT method of capacity prediction, which is based on the structural capacity of the pile, significantly under predicted the CAPWAP capacity and is not recommended for general use for project conditions similar to those analyzed in this study.

The authors recommend that during design, careful consideration be given to evaluating pile stresses and potential pile damage if IGM formations are expected at the site. It may be prudent to use a range of IGM strength parameters (parametric study) in this evaluation because of the variable nature of these materials and the real potential for excessively strong and excessively weak anomalies within the IGM deposit.

Static load testing is the only method of precisely determining the axial capacity of deep foundations. There is no substitute for good quality data. Piles can be instrumented to measure tip resistance and friction resistance along the shaft. Detailed information from accurate subsurface profiles, in-situ pressuremeter testing, and pile construction records would be valuable to assist in the development of improved design methods for deep foundations in IGMs.

IGMs are incredibly varied materials in which current geological and geotechnical knowledge provide engineers with only a limited understanding of their properties and behavior. To decrease uncertainties and thus construction costs, further research is needed in the following areas:

- develop a sampling method for IGMs that allows the collection of undisturbed samples,
- determine correlations between in-situ measurements and design parameters,
- increase mechanistic understanding of end-bearing and shaft resistance,
- conduct fully instrumented pile static load tests to compare data from in-situ tests and design methods,
- isolate shaft capacities within IGMs, and
- quantify changes that occur in IGM properties during pile installation using measured field data.

REFERENCES CITED

- AASHTO (1996). "Standard Specifications for Highway Bridges." American Association of State Highway and Transportation Officials; Washington, D.C., 16th Edition.
- Akai, K. (1993). "Testing Methods for Indurated Soils and Soft Rocks- Interim Report." *Geotechnical Engineering of Hard Soils-Soft Rocks: Proceedings of an International Symposium for ISSMFE, IAEG and ISRM in Athens, Greece, September 1993, 1707-1737.* A. A. Balkema.
- Albuquerque, P. J. R. and D. de Carvalho (2000). "Dynamic Load Test and Elastic Rebound Analysis for Estimation of the Bearing Capacity of Piles in Residual Soil." *Proceedings of the 6th International Conference on the Application of Stress-Wave Theory to Piles: Sao Paulo, Brazil; 667-681.*
- Allen, T. (2007). "Development of New Pile-Driving Formula and Its Calibration for Load and Resistance Factor Design." *Transportation Research Record: Journal of the Transportation Research Board.* No. 2004; 20-27.
- Baker, V. A., N. A. Thomsen, C. R. Nardi and M. J. Talbot. (1984). "Pile Foundation Design Using Pile Driving Analyzer." *Analysis and Design of Pile Foundations.* Eds. Joseph Ray Meyer. New York: American Society of Civil Engineers. 119-137.
- Briaud, J. and L. M. Tucker. (1984). "Residual Stresses in Piles and the Wave Equation." *Analysis and Design of Pile Foundations.* Eds. Joseph Ray Meyer. New York: American Society of Civil Engineers. 119-137.
- Brouillette, R. P., R. E. Olsen and J. R. Lai. (1993). "Stress-Strain characteristics of Eagle Ford Shale." *Geotechnical Engineering of Hard Soils-Soft Rocks: Proceedings of an International Symposium for ISSMFE, IAEG and ISRM in Athens, Greece, September 1993, 397-404.* A. A. Balkema.
- Bustamante, M., L. Ganeselli and C. Schreiner (1992). "Comparative Study on the Load Bearing Capacity of Driven Steel H-Piles in a Layered Marl." *Proceedings of the 4th International Conference on the Application of Stress-Wave Theory to Piles: the Hague, Netherlands; 531-536.*
- Bustamante, M. and H. Weber (1988). "Dynamic and Static Measurements of Steel H-Pile Capacities." *Proceedings of the 3rd International Conference on the Application of Stress-Wave Theory to Piles: Vancouver, British Columbia, Canada; 579-590.*
- Campos, J. O., A. B. Paraguassu, L. Dobereiner, L. Soares and E. B. Frazao. (1993). "The Geotechnical Behavior of Brazilian Sedimentary Rocks." *Geotechnical Engineering of Hard Soils-Soft Rocks: Proceedings of an International*

Symposium for ISSMFE, IAEG and ISRM in Athens, Greece, September 1993, 69-84. A. A. Balkema.

Cannon, J. G. (2000). "Case-Study on the Application of High Strain Dynamic Pile Testing to Non-Uniform Bored Piles." Proceedings of the 6th International Conference on the Application of Stress-Wave Theory to Piles: Sao Paulo, Brazil; 399-402.

CAPWAP (2006). Case Pile Wave Analysis Program, version 2006. Computer software by Pile Dynamics, Inc.

CDOT (2005). "Colorado Department of Transportation Standard Specifications: Road and Bridge Construction."

Chapman, G. A. and J. P. Wagstaff (1992). "Predictions of Pile Performance Using Dynamic Testing." Proceedings of the 4th International Conference on the Application of Stress-Wave Theory to Piles: The Hague, Netherlands; 537-543.

Cheng, S. S. and S. A. Ahmad (1988). "Dynamic Testing versus Static load Test: Five Case Histories." Proceedings of the 3rd International Conference on the Application of Stress-Wave Theory to Piles: Vancouver, British Columbia, Canada; 477-489.

Chow, Y. K., K. Y. Wong, G. P. Karuanaratne and S. L. Lee. (1988). "Estimation of Pile Capacity from Stress-Wave Measurements." Proceedings of the 3rd International Conference on the Application of Stress Wave theory to Piles: Vancouver, British Columbia, Canada; 626-634.

Clarke, B. G. and A. Smith (1993). "Self-Boring Pressuremeter Tests in Weak Rocks." *The Engineering Geology of Weak Rock*: Proceedings of the 26th Annual Conference of the Engineering Group Geological Society in Leeds, UK, September 1990; 233-241.

Corte, J. F. and M. Bustamante (1984). "Experimental Evaluation of the Determination of Pile Bearing Capacity from Dynamic Tests." Proceedings of the 2nd International Conference on the Application of Stress-Wave Theory to Piles: Stockholm, Sweden; 17-24.

Cripps, J. C, and R. K. Taylor. (1981). "The Engineering Properties of Mudrocks." *The Quarterly Journal of Engineering Geology*. Volume 14: pp. 325-346.

Das, B. M. (2005). Principles of Foundation Engineering. 5th Edition.

de Freitas, H. (1993). "Introduction to Session 1.2: Weak Arenaceous Rock." *The Engineering Geology of Weak Rock*: Proceedings of the 26th Annual Conference

- of the Engineering Group Geological Society in Leeds, UK, September 1990, 115-123.
- Dobereiner, L. and M. H. de Freitas. (1986). "Geotechnical Properties of Weak Sandstones." *Geotechnique*. Volume 36 (March 1986), Issue 1: pp.79-94.
- DRIVEN (2001). Computer software by the Federal Highway Administration, ver. 1.2.
- El-Sohboy, M. A., S. O. Mazen and M. I. Aboushook. (1993). "Geotechnical Aspects on Behavior of Weakly Cemented and Over-consolidated Soil Formations." *Geotechnical Engineering of Hard Soils-Soft Rocks: Proceedings of an International Symposium for ISSMFE, IAEG and ISRM in Athens, Greece, September 1993*, 91-104. A. A. Balkema.
- Fellenius, B. H (1988). "Variation of Capacity within a Pile Group as Determined by Dynamic Testing." Proceedings of the 3rd International Conference on the Application of Stress-Wave Theory to Piles. Fellenius editor, Balkema, Ottawa, Canada; May 25-27, pp. 826-829.
- Fellenius, B. H., R. D. Edde and L. L. Beriault. (1992). "Dynamic and Static Testing for Pile Capacity in a Fine-Grained Soil." Proceedings of the 4th International Conference on the Application of Stress-Wave Theory to Piles: The Hague, Netherlands; 401-408.
- FHWA Driven Pile Manual. (2006). *Design and Construction of Driven Pile Foundations Reference Manual*. Federal Highway Administration Publication, FHWA-NHI-05-042 and FHWA-NHI-05-043, Volumes I and II.
- Finno, R. J. and E. R. Budyn. (1988). "Panel Report: Design Parameters for Drilled Shafts in Intermediate Geomaterials." *The Geotechnics of Hard Soils-Soft Rocks Proceedings of the 2nd International Symposium on Hard Soils, Soft Rocks in Naples, Italy, October 1988*, 35-40. A. A. Balkema.
- Gannon, L. A., G. G. T. Masterton, W. A. Wallace and D. Muir Wood. (1999). Piled Foundations in Weak Rock. London: Ciria.
- Gerwick, B. C. (2004). "Pile Installation in Difficult Soils" *Journal of Geotechnical and Geoenvironmental Engineering*. Volume 130, Issue 5: pp.454-460.
- Gravare, C. J. and I. Hermansson (1980). "Practical Experiences of Stress-wave Measurements." Proceedings of the 1st International Conference on the Application of Stress-Wave Theory to Piles: The Hague, Netherlands; 99-120.
- GRLWEAP (2005). Computer software by Pile Dynamics, Incorporated.

-
- Hartung, M., K. Meier and W. Rodatz (1992). "Dynamic Pile Test on Sheet Piles." Proceedings of the 4th International conference on the Application of Stress-Wave Theory to Piles: The Hague, Netherlands; 259-264.
- Holeyman, A., J. Maertens, C. Legrand and N. Huybrechts. (2000). "Results of an International Pile Dynamic Test Prediction Event." Proceedings of the 6th International Conference on the Application of Stress-Wave Theory to Piles: Sao Paulo, Brazil; 725-732.
- Holloway, D. M. and G. A. Romig (1988). "CPT and Dynamic Pile Testing in Foundation Design." Proceedings of the 3rd International Conference on the Application of Stress Wave Theory to Piles: Vancouver, British Columbia, Canada; 889.
- Holm, G. (1984). "Dynamic and Static Load Testing of Friction Piles in a Loose Sand." Proceedings of the 2nd International Conference on the Application of Stress Wave Theory to Piles: Stockholm, Sweden; 240-243.
- Huang, S. M. (1988). "Application of Dynamic measurement on Long H-Pile Driven into Soft Ground in Shanghai." Proceedings of the 2nd International Conference on the Application of Stress-Wave theory to Piles: Stockholm, Sweden; 635-643.
- Johnston, I. W. (1989). "Discussion Leaders Report: Material Properties of Weak Rock." Proceedings of the International Conference on Soil Mechanics and Foundation Engineering in Montreal, Canada: pp. 2831-2833.
- Johnston, I. W. (1995). "Rational Determination of the Engineering Properties of Weak Rocks." *Geotechnical Engineering Advisory Panel: Proceedings of the Institution of Civil Engineers*, April 1995, 86-92.
- Klingberg, D. J. and P. Mackenzie (2000). "Static and Dynamic Testing of the 'Campile' – A Displacement, Cast-In-Situ Pile." Proceedings of the 6th International Conference on the Application of Stress-Wave Theory to Piles: Sao Paulo, Brazil; 715-718.
- Kormann, A. M., P. R. Chamecki, L. Russo Neto, L. Antoniutti Neto and G. Bernardes. (2000). "Behavior of Short CFA Piles in an Overconsolidated Clay Based on Static and Dynamic Load Tests." Proceedings of the 6th International Conference on the Application of Stress-Wave Theory to Piles: Sao Paulo, Brazil; 707-714.
- Krauter, E. (1993). "General Co-report: Geological and Geotechnical Features, Investigation and Classification of Hard Soils." *Geotechnical Engineering of Hard Soils-Soft Rocks: Proceedings of an International Symposium for ISSMFE, AEG and ISRM in Athens, Greece, September 1993*, 1819-1826. A. A. Balkema.

- Likins, G., J. Dimaggio, F. Rausche and W. Teferra. (1992). "A Solution for High Case Damping Constants in Sands." Proceedings of the Fourth International Conference on the Application of Stress Wave Theory to Piles: The Netherlands; 117-120.
- Likins, G. and Rausche, F. (2004). "Correlation of CAPWAP with Static Load Tests." Proceedings of the 7th International Conference on the Application of Stress-wave Theory to Piles: Petaling Jaya, Selangor, Malaysia; 153-165.
- Lima, H. M. (2000). "Analysis of Dynamic Load Tests on Steel Rail Piles." Proceedings of the 6th International Conference on the Application of Stress-Wave Theory to Piles: Sao Paulo, Brazil; 375-381.
- Marinos, P. G. (1997). "General Report: Hard Soils-Soft Rocks: Geological Features with Special Emphasis to Soft Rocks." *Geotechnical Engineering of Hard Soils-Soft Rocks*: Proceedings of an International Symposium for ISSMFE, IAEG and ISRM in Athens, Greece, September 1993, 1807-1818. A. A. Balkema.
- Mathias D. and M. Cribbs (1998). "DRIVEN 1.0: A Microsoft Windows Based Program for Determining Ultimate Static Pile Capacity." Federal Highway Administration.
- Matsumoto, T., K. Fujita, O. Kusakabe, M. Okahara, N. Kawabata and S. Nishimura. (2000). "Dynamic Load Testing and Statnamic Load Testing for Acceptance and Design of Driven Piles in Japan." Proceedings of the 6th International Conference on the Application of Stress-Wave Theory to Piles: Niyama and Beim editors, Balkema, Sao Paulo, Brazil; 335-345.
- Mayne, P. W. and D. E. Harris (1993). "Axial Load Displacement Behavior of Drilled Shaft Foundations in Piedmont Residuum." *FHWA Reference No. 41-30-2175*. Georgia Tech Research Corporation, Geotechnical Engineering Division, Georgia Institute of Technology, School of Civil Engineering; Atlanta.
- Nguyen. T. T., B. Berggren and S. Hansbo (1988). "A New Soil Model for Driving and Drivability Analysis." Proceedings of the 3rd International Conference on the Application of Stress-Wave Theory to Piles: Vancouver, British Columbia, Canada; 353-367.
- Oliveira, R. (1993). "Weak Rock Materials." *The Engineering Geology of Weak Rock*: Proceedings of the 26th Annual Conference of the Engineering Group Geological Society in Leeds, UK, September 1990, pp. 5-15. A. A. Balkema.
- O'Neill, M. W., Townsend, F. C., Hassan, K. M., Buller, A. and Chen, P. S. (1996). *Load Transfer for Drilled Shafts in Intermediate Geomaterials*. U. S. Department of Transportation Publication No. FHWA-RD-95-172.

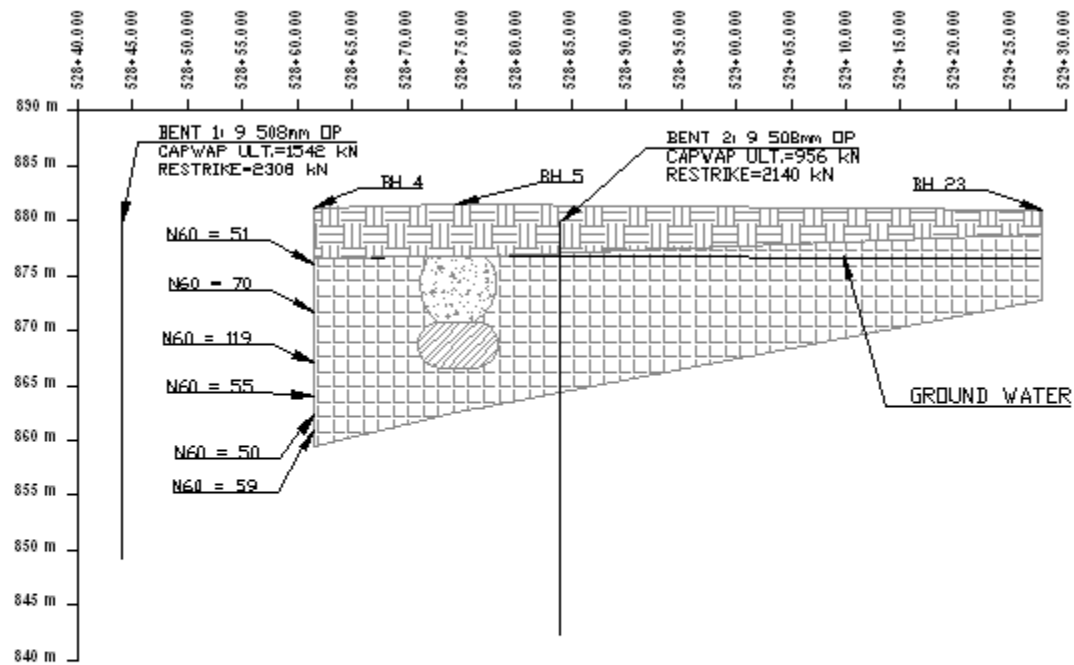
-
- Papageorgiou, O. (1993). "Soft Rocks." *Geotechnical Engineering of Hard Soils-Soft Rocks: Proceedings of an International Symposium for ISSMFE, IAEG and ISRM in Athens, Greece, September 1993, 1881-1883*. A. A. Balkema.
- Plesiotis, S. (1988). "Dynamic Testing for Highway Bridge Piling." Proceedings of the 3rd International Conference on the Application of Stress-Wave Theory to Piles; Vancouver, British Columbia, Canada; 668-678.
- Rausche, F., L. Liang, R. C. Allin and D. Rancman. (2004a). "Applications and Correlations of the Wave Equation Analysis Program GRLWEAP." Proc. 7th Intl. Conf. on the Application of Stress-wave Theory and Piles in Petaling Jaya, Selanqor, Malaysia 2004. 107-123.
- Rausche, F., B. Robinson and G. Likins. (2004b). "On the Prediction of Long Term Pile Capacity Form End-of- Driving Information." Current Practices and Future Trends in Deep Foundations, GSP No. 125 (2004): pp 77-95.
- Reeves, G. M., J. Hilary and D. Sreaton. (1993). "Site Investigations for Piled Foundations in Mercia Mudstones, Teesside, Cleveland County." *The Engineering Geology of Weak Rock: Proceedings of the 26th Annual Conference of the Engineering Group Geological Society in Leeds, UK, September 1990*, pp. 457-463. A. A. Balkema.
- Riker, R. E. and B. H. Fellenius (1992). "A Comparison of Static and Dynamic Pile Test." Proceedings of the 4th International Conference on the Application of Stress Wave Theory to Piles: The Hague, Netherlands; 143-152.
- Sanchez, Del Rio, J. (1984). "Stress-Wave Measurements of Large Raymond-Type Piles." Proceedings of the 2nd International Conference on the Application of Stress Wave Theory to Piles: Stockholm, Sweden; 221-228.
- Seidel, J. P., G. D. Anderson and N. J. Morrison (1992). "The effects of Pile Relaxation on Toe Capacity and Stiffness." Proceedings of the 4th International Conference on the Application of Stress-Wave Theory to Piles: The Hague, Netherlands; 619-626.
- Seidel, J. P., I. J. Haustorfer and S. Plesiotis (1988). "Comparison of Dynamic and Static Testing for Piles Founded into Limestone." Proceedings of the 3rd International Conference on the Application of Stress-Wave Theory to Piles: Vancouver, British Columbia, Canada; 717-723.
- Seidel, J. P. and M. Kalinowski (2000). "Pile Set-Up in Sands." Proceedings of the 6th International Conference on the Application of Stress-Wave Theory to Piles; 335-344.

-
- Seidel, J. P. and D. J. Klingberg (1992). "The Instantaneous Liquefaction of Silty Soils During Installation of Displacement Piles." Proceedings of the 4th International Conference on the Application of Stress-Wave Theory to Piles: The Hague, Netherlands; 153-158.
- Shibata A., N. Kawabata, Y. Wakiya, Y. Yoshizawa, M. Hayashi and T. Matsumoto (2000). "A Comparative Study of Static, Dynamic and Statnamic Load Tests of Steel Pile Piles Driven in Sand." Proceedings of the 6th International Conference on the Application of Stress-Wave Theory to Piles: Sao Paulo, Brazil; 583-590.
- Shioi, Y., O. Yoshida, T. Meta and M. Homma. (1992). "Estimation of bearing Capacity of Steel Pipe Pile by Static Loading Test and Stress-Wave Theory." Proceedings of the 4th International Conference on the Application of Stress-Wave Theory to Piles: The Hague, Netherlands; 325 330.
- Skov, R. and H. Denver (1988). "Time-Dependence of Bearing Capacity of Piles." Proceedings of the 3rd International Conference on the Application of Stress-Wave Theory to Piles: Vancouver, British Columbia, Canada; 879-888.
- Smith, A. E. L. (1960). "Pile Driving Analysis by the Wave Equation." *Journal of the Soil Mechanics and Foundations Division*, ASCE, vol. 86, no. SM4, August.
- Spink, T. W. and D. R. Norbury. (1993). "The Engineering Geological Description of Weak Rocks and Over-consolidated Soils." *The Engineering Geology of Weak Rock*: Proceedings of the 26th Annual Conference of the Engineering Group Geological Society in Leeds, UK, September 1990, pp. 289-301. A. A. Balkema.
- Svinkin, M. R. (2000). "Time Effect in Determining Pile Capacity by Dynamic Methods." Proceedings of the 6th International Conference on the Application of Stress-Wave Theory to Piles: Sao Paulo, Brazil; 35-40.
- Svinkin, M. R. and R. Skov (2000). "Dynamic Pile Testing and Finite Element Calculations for the Bearing Capacity of a Quay Wall Foundation - Container Terminal Altenwerder, Port of Hamberg." Proceedings of the 6th International Conference on the Application of Stress-Wave Theory to Piles: Sao Paulo, Brazil; 249-274.
- Tanimoto, C. (1982). "Engineering Experience with Weak Rocks in Japan." *Issues in Rock Mechanics*: Proceedings of the 23rd Symposium on Rock Mechanics in Berkeley, California, August 1982, pp. 999-1014. Society of Mining Engineers of the American Mining, Metallurgical and Petroleum engineers, Inc.
- Thompson, R. P. and M. Devata (1980). "Evaluation of the Ultimate Bearing Capacity of Different Piles." Proceedings of the 1st International Conference on the Application of Stress Wave Theory to Piles: The Hague, Netherlands; 163-195.

- Thompson, R. P. and Goble (1988). "High Case Damping Constants in Sand." Proceedings of the Third International Conference on the Application of Stress Wave Theory to Piles: Ottawa, Canada; 555-564.
- Wakiya, Y., O. Hashimoto, M. Fukuwaka, T. Oki, H. Shinomiya and F. Ozeki. (1992). "Ability of Dynamic Testing and Evaluation of Bearing Capacity Recovery from Excess Pore Pressure measured in the Field." Proceedings of the 4th International Conference on the Application of Stress-Wave Theory to Piles: The Hague, Netherlands; 665-670.
- Warrington, D. C. (1988). "A New Type of Wave Analysis Program." Proceedings of the 3rd International Conference on the Application of Stress-Wave Theory to Piles: Vancouver, British Columbia, Canada; 142-151.
- Yao, H. L., C. S. Shih, T. C. Kao and R. F. Wang. (1988). "Experiences of Dynamic Pile Loading Tests in Taiwan." Proceedings of the 3rd International Conference on the Application of Stress-Wave Theory to Piles: Vancouver, British Columbia, Canada; 805-813.
- Zheng, Y. M., J. M. Zheng and B. Chen (2000). "Correlation Analyses of Dynamic and Static Load Tests for Nine Piles." Proceedings of the 6th International Conference on the Application of Stress-Wave Theory to Piles: Sao Paulo, Brazil; 651-656.
- Zhou, L. B. and J. Wu (2000). "Comparative Analysis of Dynamic and Static Test of Foundation Pile." Proceedings of the 6th International Conference on the Application of Stress-Wave Theory to Piles: Sao Paulo, Brazil; 673-681.

Appendix A: Project Subsurface Profiles

(CN Q744) MEDICINE TREE



LEGEND

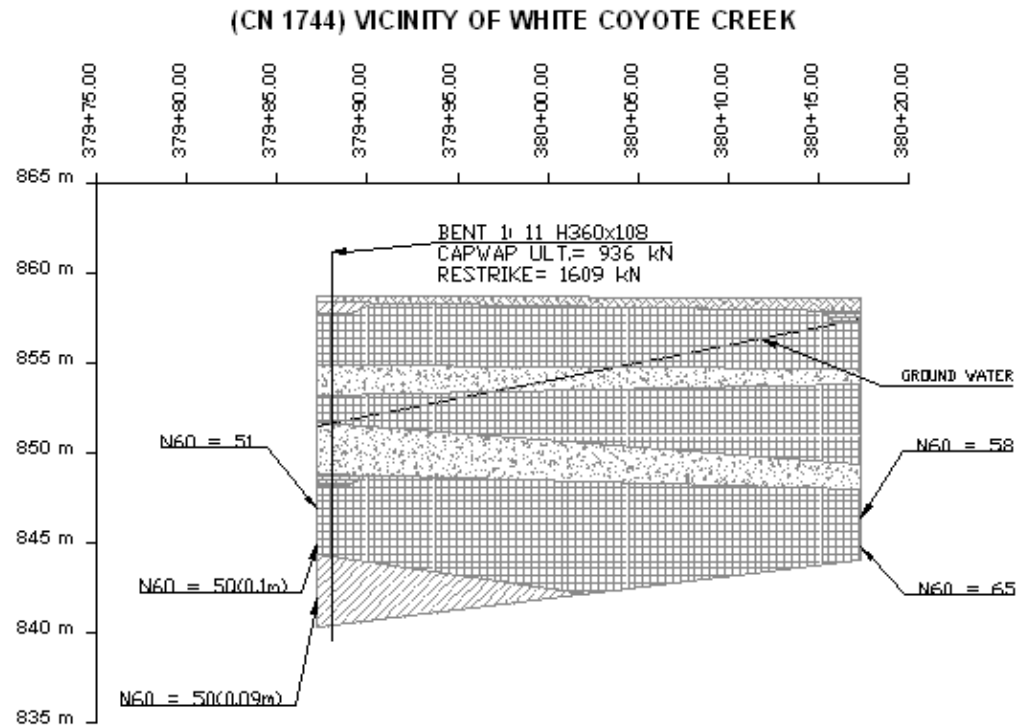
SAND	SHALE	COAL
SILT	TOPSOIL	SANDSTONE
CLAY	CLAYSTONE	PILE LOCATIONS
GRAVEL	SILTSTONE	GRAVEL FILL

PROJECT INFORMATION

NAME: Q744 MEDICINE TREE - VIC. OF RED HORN RD.
 DESCRIPTION: 1 SPAN BRIDGE
 PILES RAN
 IGM DESCRIPTION: DENSE SILTY GRAVEL

NOTE 1) GROUNDWATER LEVELS MEASURED UPON COMPLETION OF DRILLING
 2) PILE DEPTHS ARE DEPTHS OF CAPVAP ANALYSIS.
 3) N60 VALUES ARE BLOWS FOR 0.3M DISTANCE.

Figure A.1. Soil profile for project Q744 – Medicine Tree.



LEGEND

- | | | |
|--------|-----------|----------------|
| SAND | SHALE | COAL |
| SILT | TOPSOIL | SANDSTONE |
| CLAY | CLAYSTONE | PILE LOCATIONS |
| GRAVEL | SILTSTONE | GRAVEL FILL |

PROJECT INFORMATION

NAME: 1744 VICINITY OF WHITE COYOTE CREEK

DESCRIPTION: 1 SPAN BRIDGE
PILES RAN

IGM DESCRIPTION: DENSE SILTS AND GRAVELS

- NOTE: 1) GROUNDWATER LEVELS MEASURED UPON COMPLETION OF DRILLING
 2) PILE DEPTHS ARE DEPTHS OF CAPWAP ANALYSIS
 3) N60 VALUES ARE EITHER THE NUMBER OF BLOWS WITHIN 0.3m OR 50 BLOWS OVER THE GIVEN DISTANCE.

Figure A.2. Soil profile for project 1744 (Vicinity of White Coyote Creek) main structure.

(CN 2144) Porcupine Creek Bridge - Main Structure

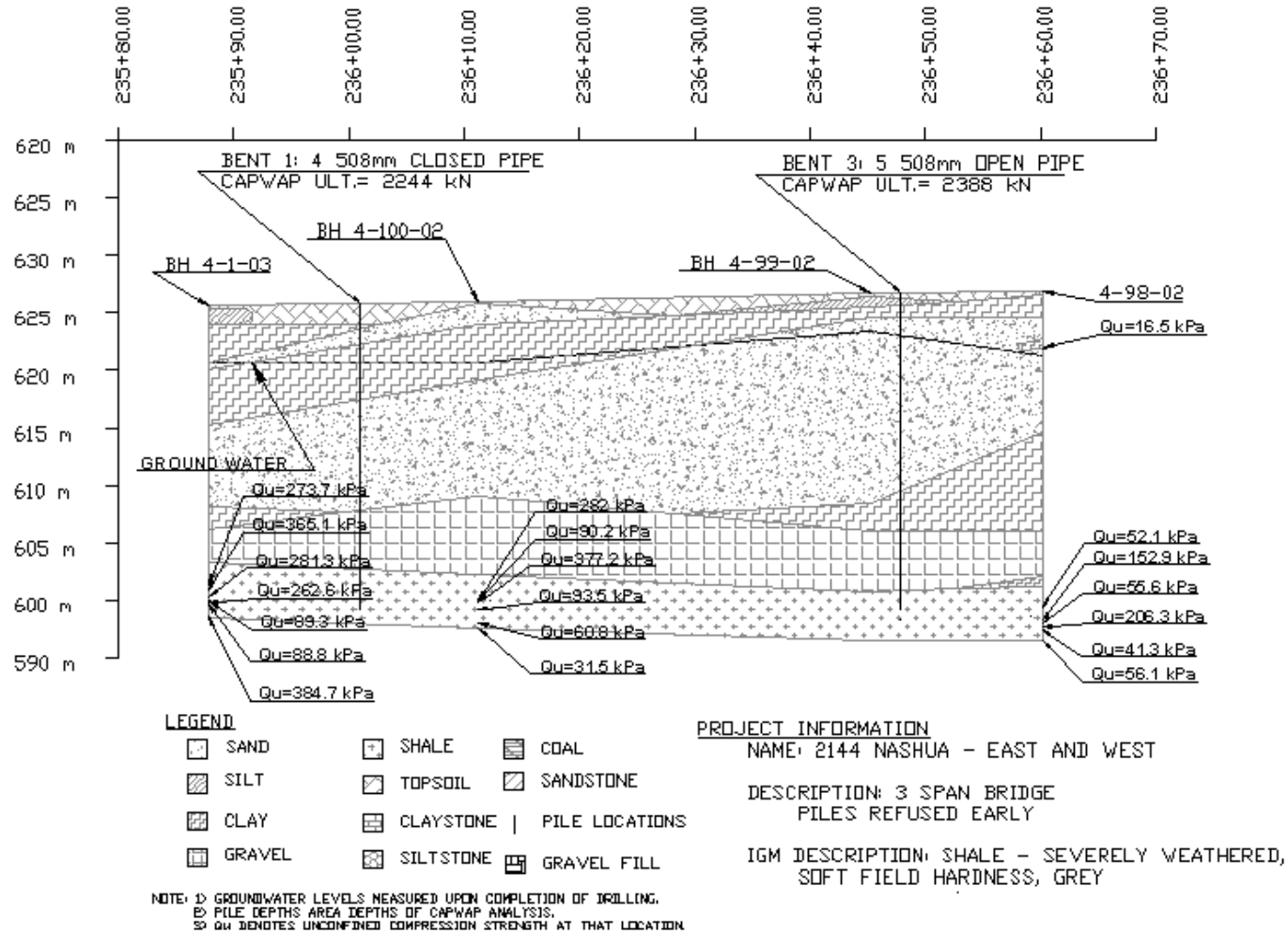


Figure A.3. Soil profile for project 2144 (Nashua Creek) main structure.

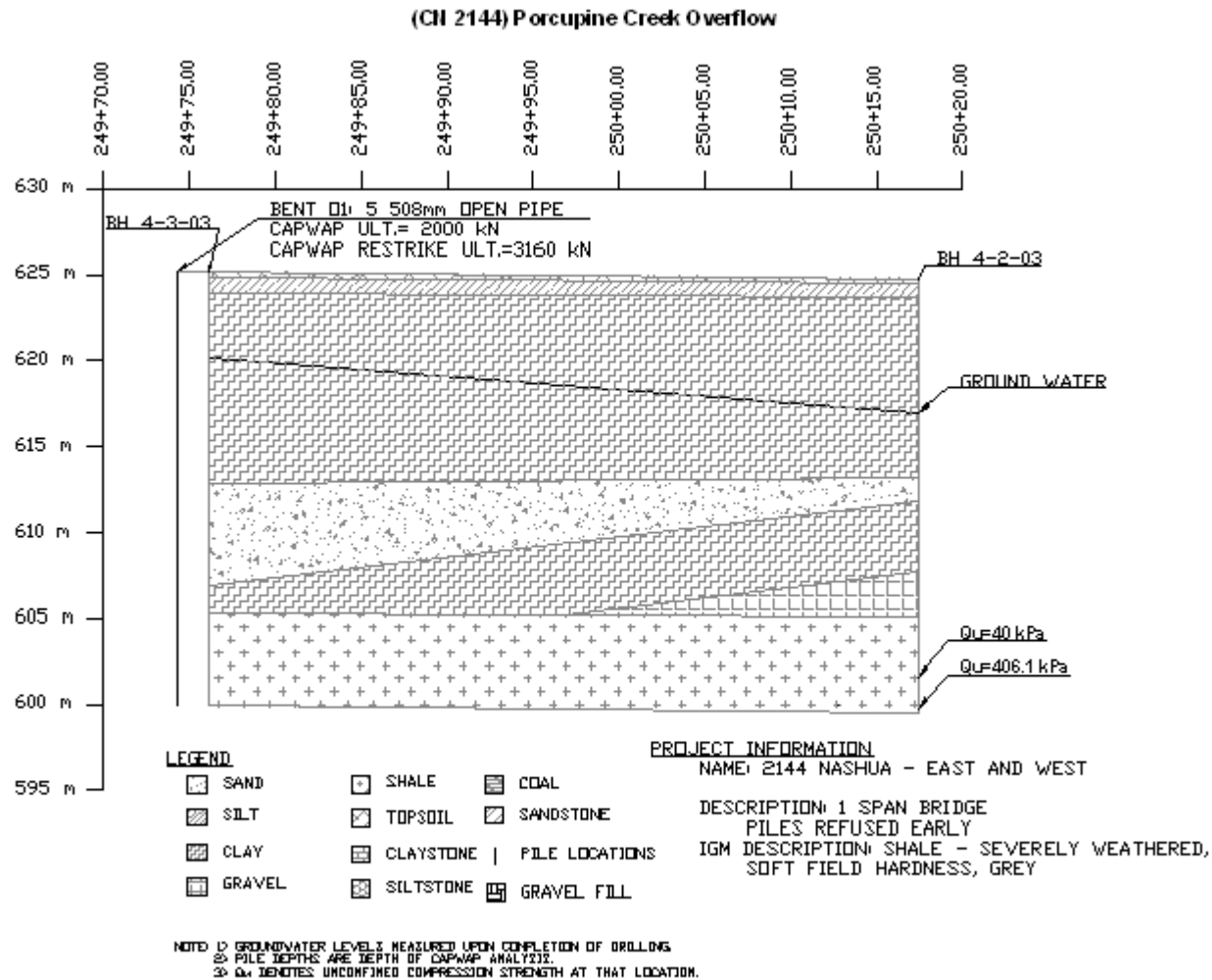


Figure A.4. Soil profile for project 2144 (Nashua Creek) overflow structure.

(CN 3417) WEST FORK POPLAR RIVER-MAIN CHANNEL

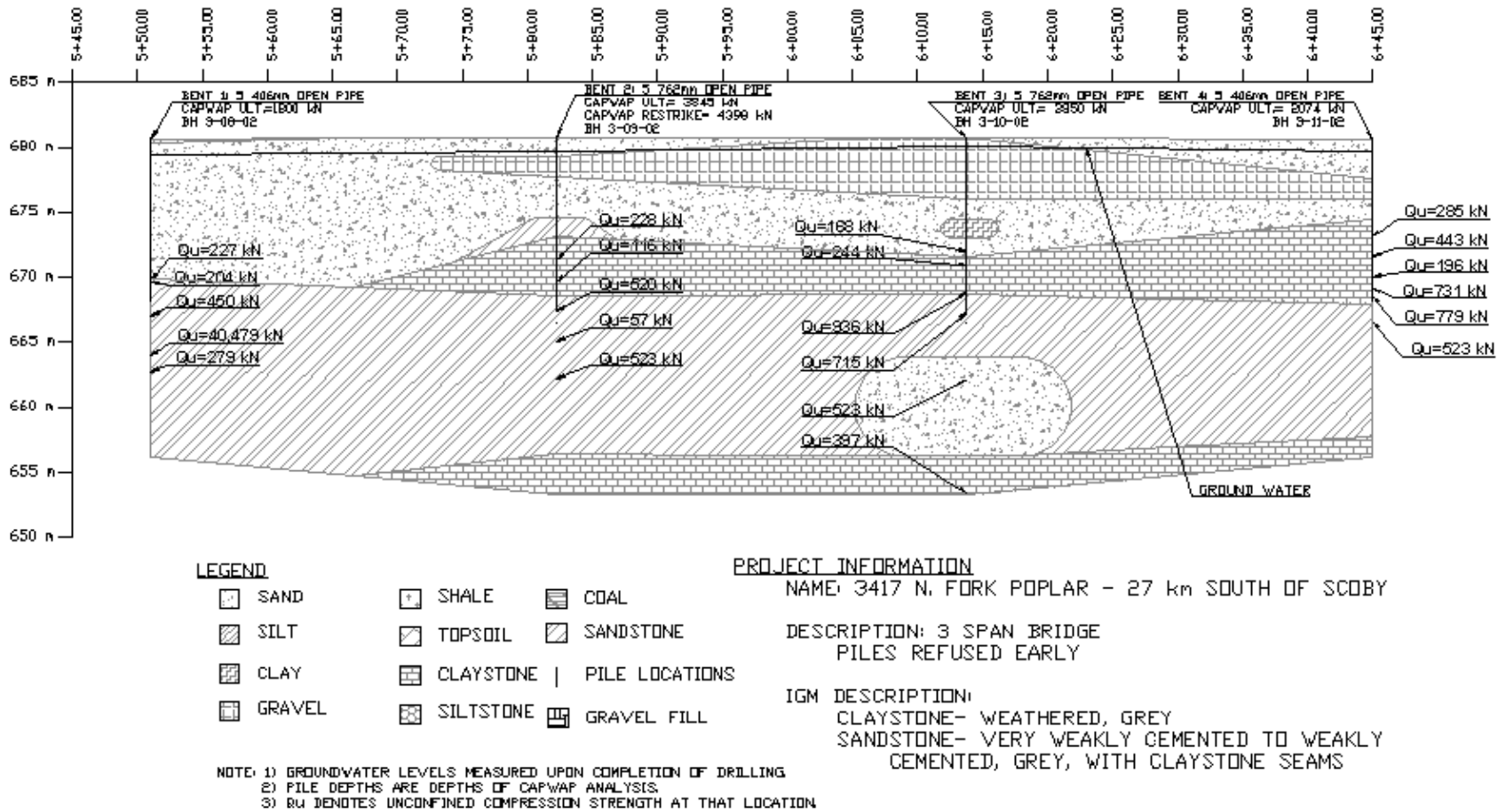


Figure A.5. Soil profile for project 3417 (West Fork Poplar River) main structure.

(CN 3417) WEST FORK POPLAR RIVER- OVERFLOW

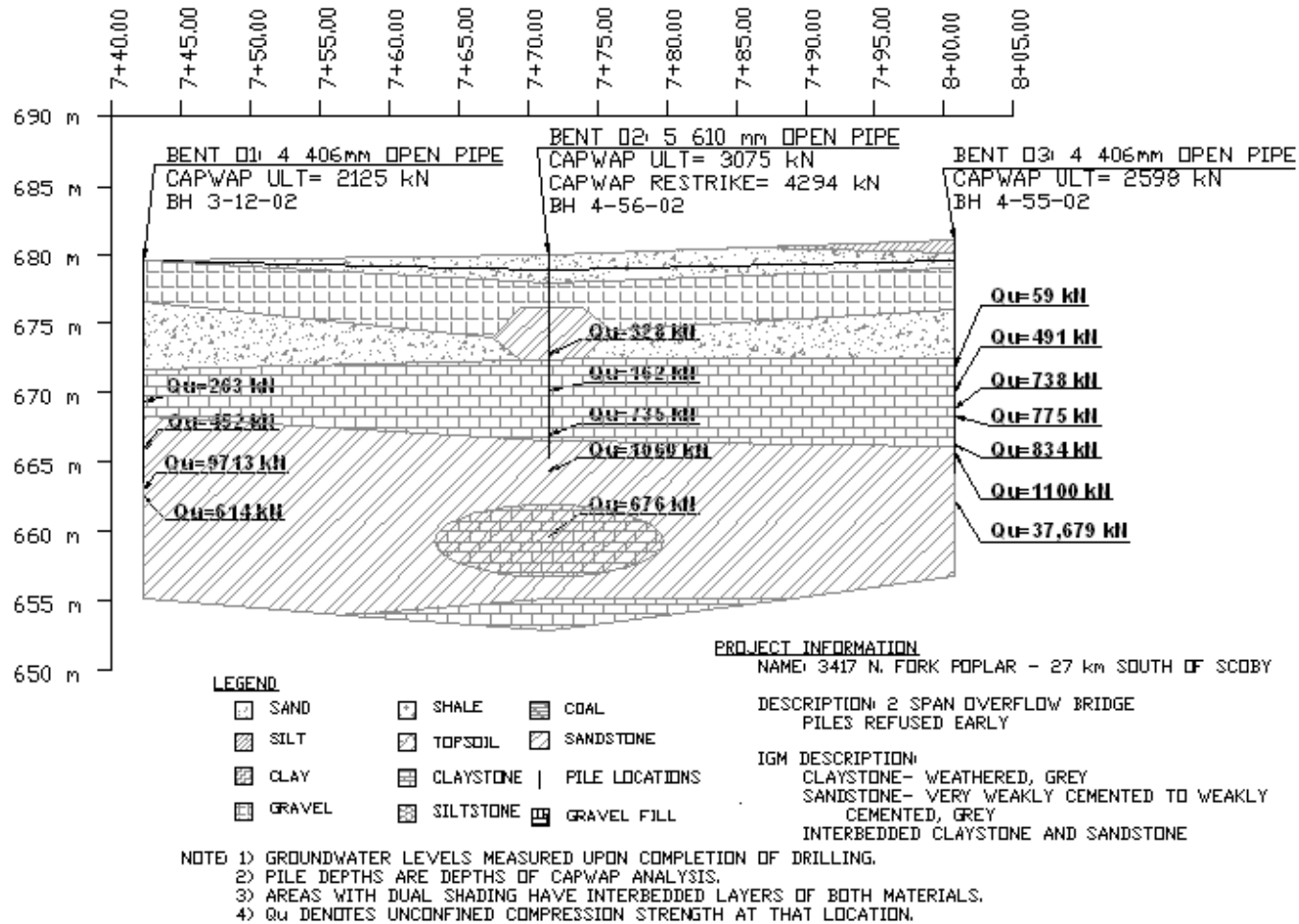


Figure A.6. Soil profile for project 3417 (West Fork Poplar River) overflow structure.

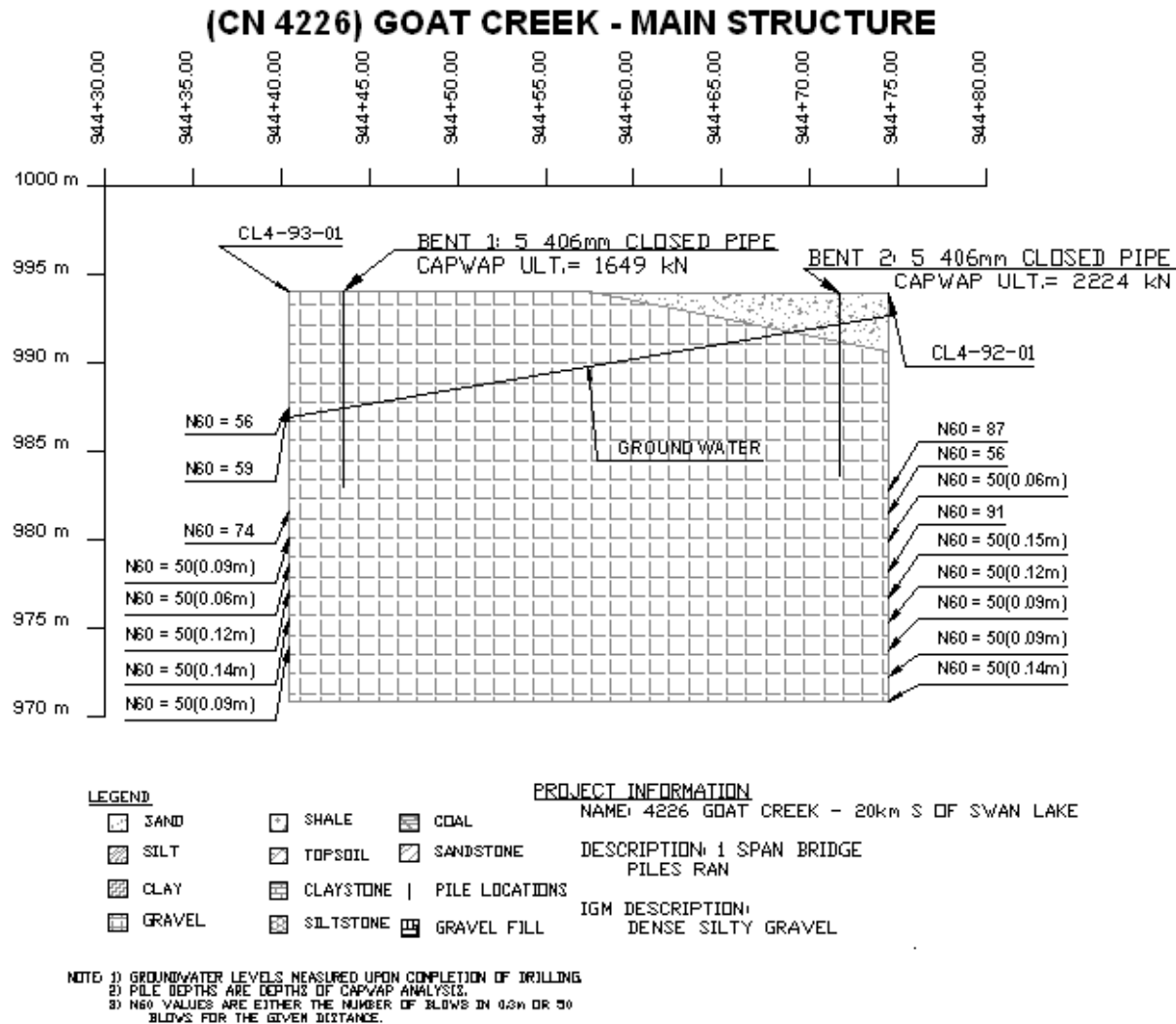


Figure A.7. Soil profile for project 4226 (Goat Creek) main structure.

(CN 4329) BIG MUDDY CREEK BRIDGE

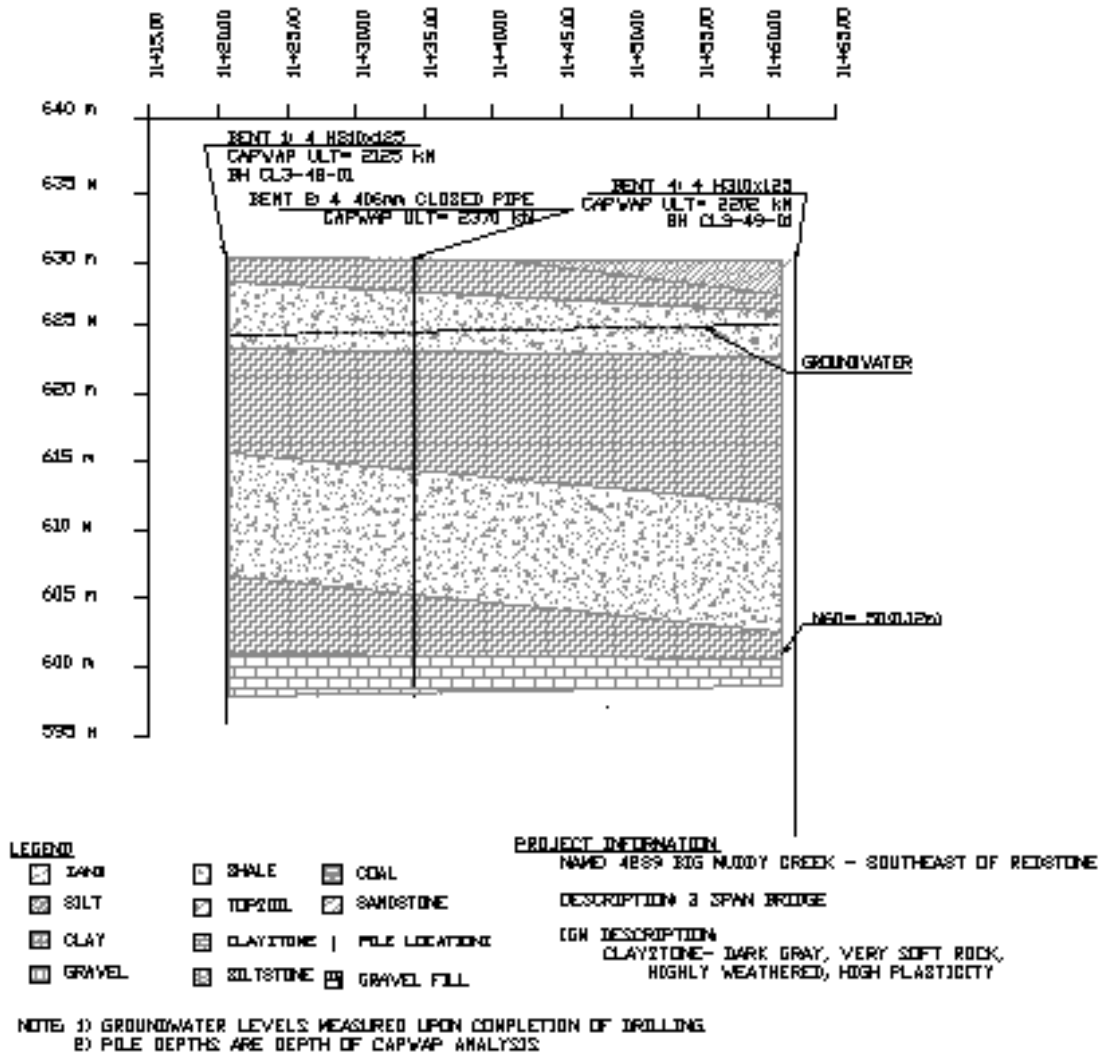


Figure A.9. Soil profile for project 4239 (Big Muddy Creek) main structure.

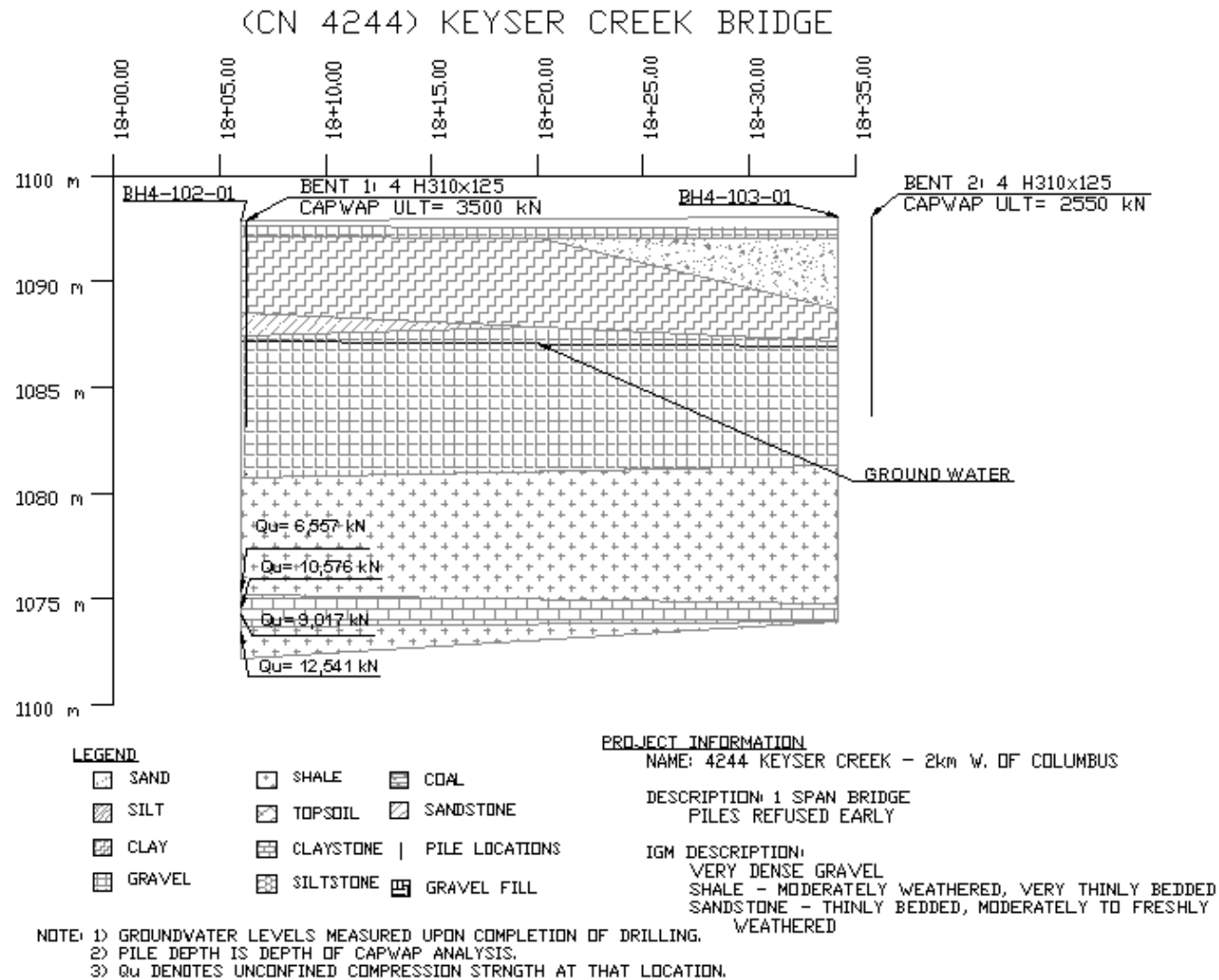


Figure A.10. Soil profile for project 4244 (Keyser Creek) main structure.

Appendix B: Compiled Project Data

Table B.1. CAPWAP Capacities and Pile Depths

Project	Bent	IGM Type	CAPWAP Cap. (kN)	CAPWAP Shaft (kN)	CAPWAP Toe (kN)	Depth in IGM (m)	Pile Pen. (m)	Layer Depth						
								1 (m)	2 (m)	3 (m)	4 (m)	5 (m)	6 (m)	7 (m)
Q744	1	CL	1542.0	1432.0	110.0	15.13	30.20	3.8	*7.3	*20.0				
	1R	CL	2308.0	2119.1	189.0	15.53	30.50	3.8	7.3	*20.0				
	2	CL	956.0	845.9	110.0	17.51	30.10	3.8	*7.3	*20.0				
	2R	CL	2140.0	1794.4	345.6	17.51	30.10	3.8	*7.3	*20.0				
	2RR	CL	2152.0	2130.3	21.5	24.58	37.50	3.8	*7.3	*20.0				
1744	1	CL	1609.2	1140.3	468.9	13.71	21.01	0.9	3.8	5.5	9.8	10.5	*14.3	*20.0
2144	1	CH	2244.0	1143.7	1100.3	4.20	26.50	6.7	15.3	*22.3	*27.7	*33.1		
	3	CH	2388.0	1791.1	596.9	1.50	27.40	18.3	20.7	*25.9	*30.0			
	O1	CH	2000.0	1694.4	305.6	4.10	25.10	12.5	18.5	*21.0	*30.0			
	O1R	CH	3160.0	2799.4	360.6	4.20	25.20	12.5	18.5	*21.0	*30.0			
3417	1	CH	1800.0	1315.1	484.9	9.35	12.40	*3.0	*16.2					
	2	CH	3845.0	2940.7	904.3	7.20	13.30	*6.1	*12.2	*27.4				
	2R	CH	4398.0	3454.4	943.6	7.30	13.40	*6.1	*12.2	*27.4				
	3	CH	3850.0	3176.7	673.3	7.40	13.50	*6.1	*12.2	*27.4				
	4	CH	2074.0	1505.7	568.3	5.39	12.40	*7.0	*13.1	*24.4				
	O1	CH	2125.0	1838.2	286.8	9.30	16.00	*6.7	*10.2	*13.6	*22.4			
	O2	CH	3075.0	2877.0	198.0	10.90	14.60	*3.7	*7.5	*13.4	*23.0			
	O2R	CH	4294.0	4094.8	199.2	10.90	14.60	*3.7	*7.5	*13.4	*23.0			
O3	CH	2598.0	2212.7	385.3	7.30	16.80	4.0	*9.5	*15.9	*23.0				
4226	1	CL	1649.0	191.0	1458.1	0.51	9.30	*3.3	*23.2					
4230	3	CL	3200.0	951.1	2248.9	4.58	8.58	*4.0	*20.0					
	3R	CL	4100.0	2179.7	1920.3	5.14	9.14	*4.0	*20.0					
	4	CL	3195.0	569.0	2626.0	3.23	7.23	*4.0	*16.0					
4239	1	CH	2125.0	1170.5	954.5	5.02	33.98	1.8	6.7	10.1	14.3	23.2	*28.9	*36.6
	2	CH	2370.0	406.6	1963.4	2.13	31.09	1.8	6.7	10.1	14.3	23.2	*28.9	*36.6
	4	CH	2202.0	851.0	1351.0	13.00	41.96	1.8	6.7	10.1	14.3	23.2	*28.9	*42.0
4244	1	CL	3500.0	465.1	3034.9	2.41	9.72	4.3	5.8	*7.3	*12.2	*15.2		
	2	CL	2550.0	455.5	2094.5	2.13	9.44	4.3	5.8	*7.3	*12.2	*15.2		

Notes: 1. Cells with "*" indicate IGM layer.
 2. Bolded text indicates start of IGM layer.

Table B.2. DRIVEN Inputs

Project	Bent	Qu by layer				Ground Water			Ult. Considerations			Driving Strength Loss						
		2 (kPa)	3 (kPa)	4 (kPa)	5 (kPa)	Drill. (m)	Dr./Res. (m)	Ult. (m)	Loc. Sc. (m)	LT Sc. (m)	Soft Soil (m)	1	2	3	4	5	6	7
Q744	1					3.70	3.70	3.70										
	1R					3.70	3.70	3.70										
	2					3.70	3.70	3.70										
	2R					3.70	3.70	3.70										
	2RR					3.70	3.70	3.70										
1744	1					1.10	1.10	1.10										
2144	1			206.2		0.00	0.00	0.00	0.00	0.00	15.30d							
	3			83.0		0.00	0.00	0.00	8.20	0.00	0.00							
	O1			223.1		0.00	0.00	0.00	0.00	0.00	6.00d							
	O1R			223.1		0.00	0.00	0.00	0.00	0.00	6.00d							
3417	1	293.7				1.22	1.22	0.00	0.00	0.00	0.00							
	2	197.0	366.7			1.52	1.52	0.00	2.38	3.75	0.00							
	2R	197.0	366.7			1.52	1.52	0.00	2.38	3.75	0.00							
	3	449.3	545.0			1.52	1.52	0.00	2.38	3.63	0.00							
	4	578.7	523.0			2.44	2.44	0.00	0.00	0.00	0.00							
	O1	263.0	452.0	5163.5		3.00	3.00	0.00	0.00	0.00	0.00							
	O2	328.0	457.5	868.0		1.50	1.50	0.00	1.97	0.03	0.00							
	O2R	328.0	457.5	868.0		1.50	1.50	0.00	1.97	0.03	0.00							
O3		709.0	19389.5		2.40	2.40	0.00	0.00	0.00	0.00								
4226	1					3.66	3.66	0.00	0.00	0.53	0.00							
4230	3					3.00	0.00	0.00	0.00	0.00	0.00							
	3R					3.00	0.00	0.00	0.00	0.00	0.00							
	4					3.00	0.00	0.00	0.00	0.00	0.00							
4239	1					5.79	5.79	0.00	0.00	0.00	15.24d	30		30	30		30	10
	2					5.79	5.79	0.00	0.00	0.00	15.24d	30		30	30		30	10
	4					5.79	5.79	0.00	0.00	0.00	15.24d	30		30	30		30	10
4244	1			9549.0	9796.5	1.52	1.52	1.52	0.00	6.53	0.00		50					
	2			750.0		1.52	1.52	1.52	0.00	6.53	0.00		50					

Qu = Unconfined Compression Strength

Table B.3. Unit Weight and Strength Properties

Project	Bent	Unit Weight (kN/m ³)							Original Inputs (c or phi)						
		1	2	3	4	5	6	7	1	2	3	4	5	6	7
Q744	1	22.0	20.0	21.0					30/30	122.0	40/40				
	1R	22.0	20.0	21.0					30/30	122.0	40/40				
	2	22.0	20.0	21.0					30/30	122.0	40/40				
	2R	22.0	20.0	21.0					30/30	122.0	40/40				
	2RR	22.0	20.0	21.0					30/30	122.0	40/40				
1744	1	14.0	17.0	16.0	16.5	16.0	18.0	18.0	93.6	38/38	36/36	37/37	543.9	40/40	606.2
2144	1	14.0	15.0	14.0	16.0	20.0	21.0		28/28	25.0	28/28	30.0	32/32	38/38	
	3	14.0	15.0	20.0	20.0				30/30	25.0	34/36	38/38			
	O1	14.0	15.0	20.0	20.0				50.0	28/28	50.0	36/38			
	O1R	14.0	15.0	20.0	20.0				50.0	28/28	50.0	36/38			
3417	1	19.6	20.4	150.0					30/30	36/36	191.5				
	2	19.6	19.6	20.4					33/33	100.5	36/36				
	2R	19.6	19.6	20.4					33/33	100.5	36/36				
	3	19.6	19.6	20.4					33/33	95.8	36/36				
	4	18.9	20.4	20.4					30/30	217.8	36/36				
	O1	19.0	19.6	18.0	20.0				30/30	36/36	150.0	36/40			
	O2	19.0	18.0	18.0	20.0				30/30	34/36	200.0	36/34			
	O2R	19.0	18.0	18.0	20.0				30/30	34/36	200.0	36/34			
O3	19.0	19.6	18.0	20.0				30/30	36/36	150.0	36/40				
4226	1	15.0	19.0						32/32	40/40					
4230	3	14.0	19.0						28/28	40/40					
	3R	14.0	19.0						28/28	40/40					
	4	14.0	19.0						28/28	40/40					
4239	1	18.9	17.3	19.2	19.5	18.1	20.0	22.8	95.8	28.1/28	23.9	23.9	28.1/28	191.5	95.8
	2	18.9	17.3	19.2	19.5	18.1	20.0	22.8	95.8	28.1/29	23.9	23.9	28.1/29	191.5	95.8
	4	18.9	17.3	19.2	19.5	18.1	20.0	22.8	95.9	28.1/31	23.9	23.9	28.1/31	191.5	95.8
4244	1	19.1	19.1	22.0	22.4	18.9			0/0	0.0	34/34	36/36	191.5		
	2	19.1	19.1	22.0	22.4	18.9			0/0	0.0	34/34	36/36	191.5		

Table B.4. GRLWEAP Parameters and Pile Information

Project	Bent	Hammer	Cushion						Pile							
			Area (cm ²)	E (MPa)	Thick (mm)	COR	Stiff.	Helmet (kN)	Length (m)	Pen. (m)	Area (cm ²)	Toe Area (cm ²)	Perim. (m)	O/C	Size (mm)	Shell (mm)
Q744	1	I-42S	2568.0	1206.0	50.8	0.92	0	12.45	32.00	30.17	100.07	100.07	1.60	O	508	12.7
	1R	I-42S	2568.0	1206.0	50.8	0.92	0	12.45	32.00	30.50	100.07	100.07	1.60	O	508	12.7
	2	I-42S	2568.0	1206.0	50.8	0.92	0	12.45	32.19	30.11	100.07	100.07	1.60	O	508	12.7
	2R	I-42S	2568.0	1206.0	50.8	0.92	0	12.45	32.19	30.25	100.07	100.07	1.60	O	508	12.7
	2RR	I-42S	2568.0	1206.0	50.8	0.92	0	12.45	32.19	37.49	100.07	100.07	1.60	O	508	12.7
1744	1	I-42S	2568.0	1206.0	50.8	0.92	0	9.71	30.38	21.01	1283.66	138.00	1.43		360x108	
2144	1	D46-32	3168.0	1207.0	127.0	0.95	0	20.92	28.04	26.50	2026.83	100.07	1.60	O	508	12.7
	3	D46-32	3168.0	1207.0	127.0	0.95	0	20.92	29.87	27.40	2026.83	100.07	1.60	O	508	12.7
	O1	D46-31	3168.0	1207.0	127.0	0.95	0	20.92	26.60	25.10	2026.83	100.07	1.60	O	508	12.7
	O1R	D46-32	3168.0	1207.0	127.0	0.95	0	20.92	26.60	25.20	2026.83	100.07	1.60	O	508	12.7
3417	1	I-30	2565.0	1210.0	63.5	0.92	0	14.03	13.50	12.40	1294.62	79.73	1.28	C	406	12.7
	2	I-80	3165.0	1210.0	63.5	0.92	0	20.36	15.24	13.30	4560.37	225.17	2.39	O	762	19.1
	2R	I-80	3165.0	1210.0	63.5	0.92	0	20.36	15.24	13.40	4560.37	225.17	2.39	O	762	19.1
	3	I-80	3165.0	1210.0	63.5	0.92	0	20.36	15.24	13.50	4560.37	225.17	2.39	O	762	19.1
	4	I-30	2565.0	1210.0	63.5	0.92	0	14.03	13.50	12.40	1294.62	79.73	1.28	O	406	12.7
	O1	I-30	2565.0	1210.0	63.5	0.92	0	14.03	17.80	16.00	1294.62	79.73	1.28	O	406	12.7
	O2	I-80	3165.0	1210.0	63.5	0.92	0	20.36	15.85	14.60	2922.47	179.68	1.92	O	610	19.1
	O2R	I-81	3165.0	1210.0	63.5	0.92	0	20.36	15.85	14.60	2922.47	179.68	1.92	O	610	19.1
4226	1	I-42S	2568.0	1206.0	50.8	0.92	0	12.45	9.30	9.30	1294.62	79.73	1.28	C	406	12.7
	3	D46-32	3168.0	1207.0	127.0	0.95	0	20.92	12.27	8.58	2922.47	180.15	1.92	O	610	19.1
4230	3R	D46-32	3168.0	1207.0	127.0	0.95	0	20.92	12.27	9.14	2922.47	180.15	1.92	O	610	19.1
	4	D46-32	3168.0	1207.0	127.0	0.95	0	20.92	10.10	7.23	1294.62	79.73	1.28	O	406	12.7
	1	D25-32	1464.5	3654.0	50.8	0.80	0	8.45	50.52	33.98	973.44	159.00	1.25		310X125	
4239	2	D25-32	2677.4	3654.2	50.8	0.80	0	15.12	33.68	31.09	1294.62	79.73	1.28	C	406	12.7
	4	D25-32	1464.5	3654.0	50.8	0.80	0	8.45	50.52	41.96	973.44	159.00	1.25		310X125	
4244	1	I-42S	2568.0	1206.0	50.8	0.92	0	9.71	15.39	9.72	973.44	159.00	1.25		310X125	
	2	I-42S	2568.0	1206.0	50.8	0.92	0	9.71	15.39	9.44	973.44	159.00	1.25		310X125	

Table B.5. Final Driving Information from CAPWAP Reports

Project	Bent	Final BC (BL/.3m)	Stroke (m)	Damping		Quake	
				Shaft (sec/m)	Toe (sec/m)	Shaft (mm)	Toe (mm)
Q744	1	62	3.1	0.351	0.499	2.667	2.972
	1R	57	3.1	0.351	0.499	2.667	2.972
	2	54	2.7	0.279	0.299	2.540	2.540
	2R	118	2.5	0.279	0.299	2.540	2.540
	2RR	133	2.8	0.279	0.299	2.540	2.540
1744	1	59	2.6	0.150	0.490	2.540	5.000
2144	1	29	2.7	0.600	0.500	3.500	3.000
	3	31	2.7	0.600	0.400	2.500	2.000
	O1	29	2.5	0.650	0.400	2.000	2.000
	O1R	59	1.2	0.650	0.400	2.000	2.000
3417	1	19	2.9	0.450	0.250	1.500	11.000
	2	30	2.3	0.400	1.030	2.500	6.600
	2R	46	2.6	0.400	1.030	2.500	6.600
	3	33	2.3	0.400	1.030	2.500	6.600
	4	31	3.1	0.450	0.250	1.500	11.000
	O1	44	3.1	0.450	0.250	1.500	11.000
	O2	24	2.3	0.250	0.500	2.500	10.000
	O2R	50	2.3	0.250	0.500	2.500	10.000
	O3	56	3.2	0.450	0.250	1.500	11.000
4226	1	96	2.3				
4230	3	45	2.3	0.328	0.600	2.500	2.800
	3R	47	2.4	0.328	0.600	2.500	2.800
	4	53	2.0	0.328	0.600	2.500	2.500
4239	1	73	2.5	0.400	0.100	5.000	12.000
	2	150	2.6	0.861	0.128	1.750	13.360
	4	73	2.8	0.720	0.102	2.503	7.000
4244	1	148	3.0	0.650	0.500	2.000	1.500
	2	119	2.7	0.650	0.500	2.000	1.500

Appendix C: Comparison of Test Results from the Literature

Table C.1. CAPWAP Capacities (kN) and Static Load Test Results (kN)

Background Data		Static Capacity		Dynamic	Reference	
Soil Type	Pile Type	Ultimate	Analysis Type	CAPWAP Ultimate	Author	Date
Soil	OP 610 mm	1344		2292	Rausche et al.	2004b
Soil	PSC 610 mm x610 mm	3204		3097	Rausche et al.	2004b
Soil	PSC 406 mm x406 mm	997		378	Rausche et al.	2004b
Soil	PSC 406 mm x406 mm	961		481	Rausche et al.	2004b
Soil	PSC 356 mm x356 mm	997		627	Rausche et al.	2004b
Soil	PSC 406 mm x406 mm	2648		3453	Rausche et al.	2004b
IGM - chalk	RC 275 mm x275 mm	1800		1560	Gravare and Hermansson	1980
IGM - Glacial Till	H 310x74	3605	Dav	3200	Thompson and Devata	1980
IGM - Glacial Till	CP 305 mm	2000	Dav	1780	Thompson and Devata	1980
IGM - Glacial Till	RC 305 mm	2310	Dav	2225	Thompson and Devata	1980
soil	H 310x74	1420	Dav	1160	Thompson and Devata	1980
soil	CP 305 mm	1335	Dav	1600	Thompson and Devata	1980
soil	H 310x74	2800	Dav	2890	Thompson and Devata	1980
soil	CP 305 mm	2450	Dav	2580	Thompson and Devata	1980
soil	Timber No 14	670	Dav	620	Thompson and Devata	1980
soil	RC 305 mm	1740	Dav	1510	Thompson and Devata	1980
IGM - Stiff Marl	CP 610 mm	3900	LPC	1610	Corte and Bustamante	1984
soil	PSC 900 mm to 1680 mm	3500		3500	Sanchez	1984
soil	PSC 900 mm to 1680 mm	5000		6000	Sanchez	1984
soil	RC 270 mm	460	Dav	535	Holm	1984
soil	RC 270 mm	300	Dav	310	Holm	1984
soil	RC 270 mm	1390	Dav	1210	Holm	1984
soil	RC 270 mm	990	Dav	820	Holm	1984
soil	RC 270 mm	690	Dav	750	Holm	1984
soil	CP 508 mm	360	Dav	361	Warrington	1988
soil	CP 508 mm	576	Dav	474	Warrington	1988
soil	CP 356 mm	344	Dav	477	Warrington	1988
soil	CP 508 mm	600	Dav	457	Warrington	1988
soil	CP 508 mm	280	Dav	436	Warrington	1988
soil	CP 90 mm	90		90	Nguyen et al.	1988
soil	CP 812 mm	5250	Dav	3200	Nguyen et al.	1988
soil	CP 298 mm	2170	Dav	2183	Cheng and Ahmad	1988
soil	CP 244 mm	1020	Dav	880	Cheng and Ahmad	1988
IGM-Till	CP 244 mm	2400	Dav	2375	Cheng and Ahmad	1988
soil	CP 244 mm	1630	Dav	1527	Cheng and Ahmad	1988
IGM-Shale	CP 324 mm	1080	Dav	921	Cheng and Ahmad	1988

Table C.1. CAPWAP Capacities (kN) and Static Load Test Results (kN) – continued

Background Data		Static Capacity		Dynamic	Reference	
Soil Type	Pile Type	Ultimate	Analysis Type	CAPWAP Ultimate	Author	Date
IGM-Till	CP 324 mm	2935	Dav	2710	Cheng and Ahmad	1988
soil	PSC 400 mm	1420	Dav	1390	Thompson and Goble	1988
soil	PSC 610 mm	1760	Dav	1760	Thompson and Goble	1988
soil	PSC 500 mm	2180	Dav	1920	Thompson and Goble	1988
soil	PSC 500 mm	800	Dav	930	Thompson and Goble	1988
soil	CP 335 mm	2580	Dav	2670	Thompson and Goble	1988
soil	H 350 mm	3200	D/10	2777	Bustamante and Weber	1988
soil	H 350 mm	3700	D/10	3513	Bustamante and Weber	1988
soil	H 350 mm	5075	D/10	4966	Bustamante and Weber	1988
soil	H 350 mm	2020	D/10	1759	Bustamante and Weber	1988
soil	H 350 mm	2400	D/10	2107	Bustamante and Weber	1988
soil	H 350 mm	1800	D/10	1591	Bustamante and Weber	1988
soil	RC 280 mm	1600		1373	Chow et al.	1988
soil	H 350 mm	7250		4485	Huang	1988
IGM-Limestone	RC 355 mm	1270	BH	1200	Plesiotis	1988
IGM-Limestone	RC 450 mm	3333	BH	3166	Plesiotis	1988
IGM-Limestone	RC 450 mm	3777	BH	3666	Plesiotis	1988
IGM-Limestone	RC 450 mm	3900		3700	Seidel et al.	1988
IGM-Limestone	RC 450 mm	4200		4118	Seidel et al.	1988
IGM-Limestone	RC 450 mm	3600		3416	Seidel et al.	1988
IGM-Limestone	PSC 600 mm	6840	Dav	6301	Seidel et al.	1988
soil	PSC 600 mm	5341	Dav	4533	Yao et al.	1988
soil	PSC 600 mm	4724	Dav	4340	Yao et al.	1988
soil	CP 245 mm	1810		1807	Yao et al.	1988
soil	RC 250 mm	1250		1335	Fellenius	1988
IGM-Chalk	CP 762 mm	4850		5170	Skov and Denver	1988
soil	RC 300 mm	880		640	Skov and Denver	1988
soil	RC 350 mm	2450		2450	Skov and Denver	1988
soil	PSC 350 mm	2180		2050	Holloway and Romig	1988
soil	PSC 600 mm	2270	Max	2310	Likins et al.	1992
soil	PSC 450 mm	1666	Max	1702	Likins et al.	1992
soil	PSC 450 mm	2540		2668	Likins et al.	1992
soil	PSC 600 mm	2869		2615	Likins et al.	1992
soil	PSC 600 mm	3724		3617	Likins et al.	1992
soil	PSC 900 mm	4900		4210	Likins et al.	1992
soil	PSC 900 mm	6905		4994	Likins et al.	1992

Table C.1. CAPWAP Capacities (kN) and Static Load Test Results (kN) - continued

Background Data		Static Capacity		Dynamic	Reference	
Soil Type	Pile Type	Ultimate	Analysis Type	CAPWAP Ultimate	Author	Date
soil	PSC 510 mm	6000	Dav	3580	Riker and Fellenius	1992
soil	PSC 600 mm	4300		3830	Seidel and Klingberg	1992
soil	PSC 600 mm	4420		4000	Seidel and Klingberg	1992
soil	Sheet Pile	1100		1344	Hartung et al.	1992
soil	OP 2000 mm	32340		29400	Shioi et al.	1992
soil	CP 244 mm	2070		2390	Fellenius et al.	1992
IGM-Marl	H 350 mm	2400	D/10	2600	Bustamante et al.	1992
IGM-Marl	H 350 mm	2000	D/10	2400	Bustamante et al.	1992
soil	RC 350 mm	4000		3486	Chapman and Wagstaff	1992
IGM-Phyllite	RC 350 mm	3600		3160	Seidel et al.	1992
soil	OP 610 mm	4658.9		4922.5	Wakiya et al.	1992
soil	OP 610 mm	6762		2382.4	Wakiya et al.	1992
soil	PSC 1370 mm	1935		2450	Svinkin	2000
soil	PSC 1370 mm	2840		2880	Svinkin	2000
soil	PSC 1370 mm	3160		3480	Svinkin	2000
soil	PSC 610 mm	1841	Dav	1672	Svinkin and Skov	2000
soil	PSC 762 mm	2273	Dav	1601	Svinkin and Skov	2000
soil	H 310 mm	1400	Dav	1512	Svinkin and Skov	2000
soil	H 310 mm	1400	Dav	2002	Svinkin and Skov	2000
soil	OP 1200 mm	5500		5800	Seidel and Kalinowski	2000
soil	OP 1200 mm	18800		19400	Seidel and Kalinowski	2000
soil	OP 800 mm	4725		4530	Matsumoto et al.	2000
soil	Pipe	2165		2040	Matsumoto et al.	2000
soil	Rail	1200	D/10	1110	Lima	2000
IGM-Desnse Sand	Screw 850 mm	1500		1809	Cannon	2000
soil	CFA 600 mm	1700		2200	Cannon	2000
soil	OP 400 mm	2150	D/10	2200	Shibata et al.	2000
soil	OP 400 mm	3000	D/10	2500	Shibata et al.	2000
soil	PSC 300 mm	1900		1863	Zheng et al.	2000
soil	PSC 300 mm	1900		1881	Zheng et al.	2000
soil	PSC 300 mm	1980		2188	Zheng et al.	2000
soil	PSC 400 mm	2160		2051	Zheng et al.	2000
soil	OP 910 mm	10567		8303	Zhou et al.	2000
soil	PSC 600 mm	8453		8001	Zhou et al.	2000
soil	PSC 800 mm	5636		5448	Zhou et al.	2000

Table C.1. CAPWAP Capacities (kN) and Static Load Test Results (kN) – end of table

Background Data		Static Capacity		Dynamic	Reference	
Soil Type	Pile Type	Ultimate	Analysis Type	CAPWAP Ultimate	Author	Date
soil	PSC 180 mm	262		216	Albuquerque and Carvalho	2000
soil	CFA 350 mm	1006	VV	877	Kormann et al.	2000
soil	CFA 350 mm	1473	VV	1700	Kormann et al.	2000
soil	CFA-D 450 mm	1800		1797	Klingberg and Mackenzie	2000
soil	PSC 350 mm	1657		1779	Holeyman et al.	2000
soil	PSC 350 mm	965		919	Holeyman et al.	2000

This document was published in electronic
format at no cost.